Bioelectrochemistry 140 (2021) 107795

Contents lists available at ScienceDirect

Bioelectrochemistry

journal homepage: www.elsevier.com/locate/bioelechem

Gene electrotransfer of proinflammatory chemokines CCL5 and CCL17 as a novel approach of modifying cytokine expression profile in the tumor microenvironment

T. Bozic [a,b], G. Sersa [a,c], S. Kranjc Brezar [a], M. Cemazar [a,d,*], B. Markelc [a,c,*]

[a] Department of Experimental Oncology, Institute of Oncology Ljubljana, Zaloska cesta 2, SI-1000 Ljubljana, Slovenia
[b] Faculty of Medicine, University of Ljubljana, Vrazov trg 2, SI-1000 Ljubljana, Slovenia
[c] Faculty of Health Sciences, University of Ljubljana, Zdravstvena pot 5, SI-1000 Ljubljana, Slovenia
[d] Faculty of Health Sciences, University of Primorska, Polje 42, SI-6310 Izola, Slovenia

ARTICLE INFO

Article history:
Received 31 December 2020
Received in revised form 22 February 2021
Accepted 23 February 2021
Available online 9 March 2021

Keywords:
Chemokines
CCL5
CCL17
Cytokine expression
Gene electrotransfer
Murine tumors

ABSTRACT

The effectiveness of immunotherapy highly correlates with the degree and the type of infiltrated immune cells in the tumor tissue. Treatments based on modifying the immune cell infiltrate of the tumor microenvironment are thus gaining momentum. Therefore, the aim of our study was to investigate the effects of gene therapy with two proinflammatory chemokines CCL5 and CCL17 on inflammatory cytokine expression profile and immune cell infiltrate in two murine breast tumor models, 4T1 and E0771, and two murine colon tumor models, CT26 and MC38. *In vitro*, lipofection of plasmid DNA encoding CCL5 or CCL17 resulted in changes in the cytokine expression profile similar to control plasmid DNA, implying that the main driver of these changes was the entry of foreign DNA into the cell's cytosol. *In vivo*, gene electrotransfer resulted in high expression levels of both *Ccl5* and *Ccl17* transgenes in the 4T1 and CT26 tumor models. Besides a minor increase in the survival of the treated mice, the therapy also resulted in increased expression of *Cxcl9* and *Ifnγ*, potent activators of the immune system, in CT26 tumors. However, this was not recapitulated in changes of TME, implying that a further refinement of the dosing schedule is needed.

1. Introduction

Cancer immunotherapy is currently one of the leading scientific fields in cancer research. The involvement of patient's own immune system in the development and progression of cancer and in the outcome of treatment is a well-established paradigm [1]. The currently available immunotherapies show promising results regarding local and systemic tumor control, however some cancer patients still do not respond to the treatment [2]. Over the years, several hallmarks for successful cancer immunotherapy have been characterized, ranging from genomic predisposition of cancer cells to the specific immune cell infiltrate in the tumor microenvironment (TME) [3]. The degree and type of the infiltrated immune cells in the tumor tissue is often one of the main predictive factors that correlates with treatment outcome [4]. With the advent of multi-omics approaches, the specific differences between a responsive and non-responsive TME started to be disentangled. Moreover, with this knowledge, different strategies with the potential to convert a non-responsive TME into a responsive one could be devised [5]. Besides targeting immune checkpoints [6], strategies aiming to achieve increased infiltration of effector immune cells into tumor tissue are gaining momentum. Among them, the use of natural immune cell chemoattractants known as chemokines has also shown promising results [7].

Chemokines represent a large family of cytokines consisting of small signaling proteins, which control migration and positioning of immune and non-immune cells along their concentration gradients. Based on the position of the first two cysteine (C) residues within the protein sequence chemokines are divided into four main classes: CC–, CXC-, C- and CX3C-chemokines. Their highly conserved tertiary structural fold is the cause of multi-specificity as single chemokine generally displays affinity towards multiple chemokine receptors (CCRs) and vice versa. Chemokines have crucial role in homoestasis and disease [8]. Homeostatic chemokines regulate leukocyte maturation and migration, development, tissue repair, and angiogenesis. On the other hand, proinflammatory chemokines can generate innate and adaptive immune response at injury sites and in different pathologies, such as cancer [9].

* Corresponding authors at: Department of Experimental Oncology, Institute of Oncology Ljubljana, Zaloska cesta 2, SI-1000 Ljubljana, Slovenia.
E-mail addresses: mcemazar@onko-i.si (M. Cemazar), bmarkelc@onko-i.si (B. Markelc).

https://doi.org/10.1016/j.bioelechem.2021.107795
1567-5394/

Cells that make up the TME secrete a number of chemokines, which in turn attract different immune cell populations to the primary tumor location where they promote cancer progression through TME remodeling or elicit immune response against tumor cells [10]. Both, clinical studies as well as animal experiments indicate that certain chemokines may help the immune system to recognize and kill tumor cells [7,11].

Among proinflammatory chemokines, RANTES/CCL5 (regulated upon activation, normal T cell expressed and secreted) and TARC/CCL17 (thymus- and activation-regulated chemokine) were both associated with increased immune cell infiltration into various tumors [10,12]. Specifically, independent studies of cell migration reveled that CCL5 displays affinity to CCR1, CCR3 and CCR5, which are widely represented on the surface of CD4+ and CD8+ T lymphocytes, natural killer (NK) cells, dendritic cells (DCs) as well as tumor-associated macrophages (TAMs) [13-15]. Preclinical studies on spheroids and transgenic mouse models associated *Ccl5* overexpression in tumors with cytotoxic T lymphocyte infiltration and significant tumor growth delay in ovarian cancer [15]. Besides guiding T lymphocytes to tumor location CCL5 also participates in CD4+ helper-dependent CD8+ T lymphocyte activation [16]. Notably, the levels of CCL5 produced by NK cells originating from TME also correlate with DC accumulation, which in turn drive the antitumor immunity through antigen presentation and effector T lymphocyte activation [17,18]. Meta-analysis of a large clinical data revealed *Ccl5* and *Cxcl9* co-expression is needed for the CD8 + T lymphocyte infiltration and increased overall survival in multiple human tumors [15]. Moreover, increased CCL5 expression in triple negative breast cancer patients was associated with the recruitment of different immune cell populations [19]. Increased expression levels of *Ccl5* were also detected in brain, head and neck, liver, pancreatic, colorectal, prostate and oral cancer, which points to its potential role as a cancer biomarker [20-27]. In early breast cancer patients the increased CCL5 serum levels correlated with prolonged disease-free survival [28]. More importantly, several studies demonstrated the benefits of using CCL5 as an adjuvant for enhancing anti-tumor immunity [29].

CCL17 is expressed constitutively in thymus mainly by DCs and transiently in stimulated peripheral blood mononuclear cells, namely neutrophils and macrophages [30]. CCL17 is one of the ligands of CCR4 although affinity towards CCR8 has also been reported [12]. Both CCR4 and CCR8 are selectively expressed on T helper type 2 (Th2) and regulatory T (Treg) cells however studies show that CCR4 is the main receptor facilitating their migration [31]. Th2 cells are involved in humoral immunity while Treg cells are known for their immunosuppressive function. CCL17 signaling through CCR4 maintains the balance of these immune cells in infections, autoimmune disorders and other pathologies, including cancer [32]. However, CCL17 also plays an important role in alternative cross-priming of DCs through which they can elicit CD8+ T lymphocyte responses against cancer antigens [33]. The initial step requires interaction between activated NK cells and DCs, resulting in the production of CCL17, which guides naïve CD8+ T lymphocytes expressing CCR4 [34,35]. The effect of CCL17 on tumor growth *in vivo* was observed in murine colon cancer model, where the administration of adenoviral vector encoding CCL17 resulted in significant tumor regression and generation of specific immunity in re-challenge experiments [36]. Moreover, increased serum levels of CCL17 in advanced melanoma patients treated with dendritic cell-based immunotherapy were associated with progression-free survival [37].

Currently different clinical trials of immunomodulatory cytokines, such as IL-12 and IL-2, which showed to be effective against various tumors are in progress [38]. However, systemic delivery of recombinant cytokines or viral vectors can result in serious, potentially life-threatening, adverse effects [39-41]. By contrast, intratumoral injection of plasmid DNA followed by gene electrotransfer (GET) is a safe and effective method for local delivery of plasmid DNA encoded cytokines to tumor tissue [42-44]. Several clinical trials utilizing GET of different plasmid DNA encoded therapeutic molecules were already initiated for the treatment of different cancers [45,46]. Until now, the proinflammatory chemokines have never been studied in this setting. Thus, the combination of local delivery of plasmid DNA by GET and the immunomodulatory properties of chemokines CCL5 and CCL17 could represent a promising approach for cancer immunotherapy.

Therefore, the aim of our study was to investigate the effects of two proinflammatory chemokines CCL5 and CCL17 on TME in murine breast (4T1, E0771) and colon (CT26, MC38) cancer models. Both chemokines were separately encoded on commercially available DNA plasmids, which were transfected into tumor cells *in vitro* using lipofection and with GET *in vivo* in order to achieve their overexpression. Then, the effect of the transgene overexpression on the expression of other proinflammatory cytokines *in vitro was* determined with qRT-PCR. Furthermore, the effect of GET of plasmid DNA encoding CCL5 or CCL17 on the expression of other proinflammatory cytokines, the TME, and tumor growth was then determined in two widely studied murine tumor models, 4T1 mammary carcinoma and CT26 colon carcinoma, which differ in their baseline immunophenotype [47].

2. Materials and methods

2.1. Plasmids

The plasmids pUNO1-mcs, pUNO1-mCCL5 and pUNO1-mCCL17 were purchased from InvivoGen (Toulouse, France). All plasmids were amplified in a competent *Escherichia coli* (JM109; TFS, MA, US) and then isolated using the EndoFree Plasmid Mega (Qiagen, Hilden, Germany) kit according to manufacturer's instructions. The concentration of isolated plasmids was measured with Qubit DNA Broad Range kit (TFS, MA, US) by fluorometric quantification using Qubit 4 Fluorometer (TFS, MA, US). Plasmid quality was assessed by the 260/280 nm ratio (Epoch Microplate Spectrophotometer, BioTek, Bad Friedrichshall, Germany) and by agarose gel electrophoresis. For the experiments, all plasmids were diluted in physiological saline to a final concentration of 2 μg/μL.

2.2. Cell cultures

Two murine breast cancer cell lines, 4T1 and E0771, and two murine colon cancer cell lines, CT26 and MC38, were used in experiments *in vitro*. Cell lines 4T1 and CT26 were originally purchased from ATCC (VA, US), E0771 were obtained from CH3 Biosystems (NY, US), while the cell line MC38 was acquired from Kerafast (MA, US). Cells were cultured in a humidified incubator at 5% CO_2 and 37 °C. The 4T1, CT26 cells were cultured in Advanced RPMI 1640 (Gibco, Thermo Fisher Scientific, VA, US), while E0771 cells were cultured in Advanced RPMI 1640 supplemented with 10 mmol/L HEPES. MC38 cells were cultured in Advanced Dulbecco's modified MEM (DMEM, Gibco). All media were supplemented with GlutaMAX (100x, Gibco), 5% fetal bovine serum (FBS, Gibco), and Penicillin-Streptomycin (100x, Sigma-Aldrich, Merck, Darmstadt, Germany). The cells were routinely tested for mycoplasma infection by MycoAlert™ PLUS Mycoplasma Detection Kit (Lonza, Basel, Switzerland) and were mycoplasma free.

The murine breast and colon cancer models used in the study differ in their immunophenotype, which is an important parameter defining the treatment outcome. Although the amount of different infiltrated immune cell subsets in CT26 varies among studies, the model is defined as "hot"/inflamed tumor model with the high

number of infiltrated NK (>26%) and T lymphocytes (>18%) [47]. Among T lymphocytes, the cytotoxic T lymphocytes are predominant (>5%). The other colon cancer model used in the study - MC38, is associated with infiltration of myeloid-derived suppressor cells (MDSC; >47%). Moreover, higher levels of Th2-associated cytokines such as IL-4 and IL-10 were found in MC38 model compared to CT26, thus, the MC38 tumor model can be described as an immunosuppressive tumor model [47]. The breast cancer model E0771 is immunophenotypically similar to the CT26 model, with high CD45+ cell (70%) infiltration of which the CD8+ and CD4+ T lymphocytes each represent approximately 6%. Compared to the other tumor models, E0771 also has a unique abundance of MDSCs and M2 macrophages, which ranks this model between immunosuppressive MC38 and inflamed CT26 [48,49]. The 4T1 breast tumor model is on the other hand considered strictly immunosuppressive due to the high infiltration of Treg lymphocytes (>5%) and MDSCs (>50%). Its immunosuppressive nature also corresponds with the increased Th2-associated cytokine signaling [47]. With the selection of the aforementioned tumor models, we thus have a pairs of syngeneic immunophenotypically "inflamed" tumor model in Balb/c mice (CT26) and in C57Bl/6 mice (E0771) and a syngeneic immunophenotypically "immunosuppressive" tumor model in Balb/c mice (4T1) and in C57Bl/6 mice (MC38).

2.3. Transfection of cells

2.3.1. Cell transfection

One day before transfection 2.5×10^5 cells in 2 mL of growth medium were seeded in each well of a 6-well plate (VWR, PA, US). Transfection of cells with each pUNO1 plasmid was performed with Lipofectamine 2000 (1 mg/μL solution) (Thermo Fisher Scientific) in three biological replicates. Plasmid DNA-lipid complexes were prepared according to manufacturer's instructions in Opti-MEM medium (Gibco). After 5-minutes incubation at room temperature, 250 μL (containing 2.5 μg of plasmid DNA and 7 μL of Lipofectamine 2000) of prepared solution was added to each well. Control triplicates were treated with a solution containing only Lipofectamine 2000. Transfected cells were incubated in a humidified incubator at 5% CO_2 and 37 °C for 48 h until RNA extraction (protocol reported in 2.7).

2.3.2. Cell viability assay

One day before transfection 2×10^4 cells in 100 μL of growth medium were seeded in each well of a 96-well plate (VWR, PA, US). Transfection of cells with each pUNO1 plasmid was performed with Lipofectamine 2000 in eight biological replicates. Plasmid DNA-lipid complexes were prepared according to manufacturer's instructions in Opti-MEM medium (Gibco). After 5 min incubation at room temperature, 10 μL (containing 0.1 μg of plasmid DNA and 0.37 μL of Lipofectamine 2000) of prepared solution was added to each well. Control triplicates were treated with solution containing only Lipofectamine 2000. Transfected cells were incubated in a humidified incubator at 5% CO_2 and 37 °C. After 48 h incubation, 10 μL of Presto Blue (Thermo Fisher Scientific) reagent was added to each well, followed by 1 h incubation in a humidified incubator at 5% CO_2 and 37 °C. The fluorescence emission was measured with a microplate reader (Infinite 200, Tecan, Männedorf, Switzerland). Measured fluorescence intensity of treated groups was normalized to the control group.

2.4. Mice

Balb/c (BALB/cAnNCrl) female mice were obtained from Charles River Laboratories (MA, US). Mice were between 6 and 8 weeks old at the beginning of the experiments, weighing between 18 and 20 g. Mice were kept in a specific pathogen-free environment with 12-hour light–dark cycle at 20–24 °C with 55% ± 10% relative humidity and food and water provided *ad libitum*. The experiments were approved by the Ministry of Agriculture, Forestry and Food of the Republic of Slovenia (permission no. 34401–1/2015/43). The experimental procedures were performed in compliance with the guidelines for animal experiments of the EU directive (2010/63/EU) and ARRIVE guidelines.

2.5. Gene electrotransfer procedure

Mice were randomly divided into experimental groups of 6–10 animals. One day prior to the experiment, the back of the mice was shaved. Tumors were grown on the back of the mice after subcutaneous inoculation of 3×10^5 CT26 or 4T1 cells in 100 μL of 0.9% NaCl saline. The treatment was performed when the tumor volume reached 50 mm^3. Tumor volume was measured using a Vernier caliper and then calculated with a formula for ellipsoid ($a \times b \times c \times \pi/6$; where a, b and c are orthogonal tumor diameters). During the treatment, mice were under 2% (v/v) of isoflurane anesthesia (Isoflurane; Piramal Healthcare UK Limited, London, UK). The treatment was carried out by intratumoral injection of 50 μg (25 μL of 2 μg/μL plasmid DNA) of the pUNO1 empty control plasmid (pDNA Ctrl) or pUNO1 plasmid encoding either CCL5 or CCL17 using an insulin syringe. After a 5-minutes delay gene electrotransfer was performed on tumors by the application of electric pulses. Two different pulsing protocols for gene electrotransfer were used. The first one was the standard electroporation pulsing protocol used in clinics for electrochemotherapy, which is a safe and effective local ablative technique where electric pulses are used to enhance the uptake of cytotoxic drugs into the tumor cells (ECT pulses, Fig S1A, B) [50,51]. This protocol was chosen because short, high voltage electric pulses are already successfully used for gene therapy with plasmid DNA encoding human IL-12 in clinical trials [52,53]. The second pulsing protocol was adapted from Forjanic *et al* [54] and comprised of four trains of pulses, each train comprising from one high voltage (HV) and one low voltage (LV) pulse (HV-LV pulsing protocol) (Fig S1A, C). The pulses were generated by ELECTRO Cell B10 electric pulse generator (Leroy biotech, France). The pulses were delivered using 6 mm parallel stainless-steel plate electrodes. During gene electrotransfer a Conductive gel (Gel G006 ECO, FIAB, Vicchio, Italy) was used at the contact of the electrodes and the skin overlaying tumors to ensure good conductivity. To compare the transfection efficiency of GET using either ECT or HV-LV pulses plasmid pEGFP-N1 (Clontech Laboratories, Inc., Mountain View, CA, USA) encoding enhanced green fluorescent protein (EGFP) (25 μL of 2 μg/μL plasmid DNA) was used.

After the treatment tumor growth was measured three times per week in order to determine the antitumor effect. When tumor volume reached 500 mm^3 mice were euthanized. Tumor volume of 500 mm^3 was counted as a humane end point for the construction of the Kaplan-Meier curves. Tumor growth delay was calculated as the difference in time when tumors doubled in volume between the control group and the treated group. Additionally, the weight of the mice and their behavior was assessed using the mouse grimace scale (MGS) [55] as an indicator of systemic toxicity of the therapy.

2.6. Tumor collection

On days two (tumors transfected with a plasmid encoding EGFP), three and seven (tumors transfected with pUNO1 plasmids and control, non-treated tumors) after the treatment, the tumors were collected for gene expression analysis and immunofluorescence staining. Mice were euthanized and tumors were surgically removed. Immediately after, one-half of the collected tumor was weighted and frozen in liquid nitrogen. Frozen tumor samples

were crushed using a pestle and then stored at −80℃ before RNA extraction. The other half of the tumor was first fixed in 4% paraformaldehyde (PFA; Alfa Aesar) overnight, then incubated in 30% sucrose for 24 h, embedded in Optimal cutting temperature compound (OCT compound) and snap-frozen in liquid nitrogen.

2.7. RNA extraction

RNA was extracted from treated cells and tumors using Total RNA Kit, peqGOLD (VWR) according to the manufacturer's instructions. In the *in vitro* experiments, cell lysis was performed with 400 uL of the enclosed TRK Lysis buffer, while in the case of tumors the TRI Reagent (Thermo Fisher Scientific) was used. The total RNA concentration was determined with Qubit DNA Broad Range kit by fluorometric quantification using Qubit 4 Fluorometer (Thermo Fisher Scientific).

2.8. Gene expression analysis

First strand cDNA was generated from 2 μg of template RNA using a Thermocycler Primus 25 (Peqlab, UK) and SuperScript VILO cDNA Synthesis Kit (Thermo Fisher Scientific) in a 20 μL reaction mix, according to the manufacturer's instructions. Priming was performed at 25℃ for 10 min and reverse transcription for 60 min at 42℃. The cDNA was then stored at −20℃ for subsequent analysis. Quantitative Polymerase Chain Reaction was performed with QuantStudio 3 Real-Time PCR System (Thermo Fisher Scientific). The samples were prepared using SYBR PowerUp Master Mix (Thermo Fisher Scientific) and predesigned chemokine and cytokine specific primers (IDT, IA, US) (Table S1). To determine transfection efficiency, the samples were prepared using TaqMan Gene Expression Master Mix (Applied Biosystems, Thermo Fisher Scientific) and TaqMan Gene Expression Assay (Applied Biosystems, Life Technologies) for EGFP (Mr04097229_mr) and murine GAPDH (Mm99999915_g1) for internal control, as described previously [56]. Briefly, the standard thermocycling program consisted of a 95℃ denaturation for 2 min, followed by 40 cycles of 95℃ for 15 s and 60℃ for 60 s. All samples were run in duplicates and the products were analyzed on QuantStudio™ 3 Real-Time PCR System (Thermo Fisher Scientific). Relative quantification was performed by comparison to the housekeeping genes β-actin (*Ba*) in *in vitro* experiments, glyceraldehyde 3-phosphate dehydrogenase (*Gapdh*) in *in vivo* experiments where expression of EGFP was determined, and RNA polymerase II subunit A (*Polr2a*) in the rest of *in vivo* experiments. Reactions with the template free control were included for each set of primers on each plate.

2.9. Immunofluorescence

Fourteen-micrometer thick frozen tissue sections were prepared using Leica CM1850 cryostat and stained with primary (Table S2) and secondary (Table S3) antibodies. Staining was performed by first drying the sections for 10 min at 37 °C and then washing them twice for 5 min in 1X PBS. Antigen retrieval was then performed by putting the slides in a hot citrate buffer (approx. 95 °C) which was cooled down on air, at room temperature (RT) for 30 min followed by a 30 min cooling in RT water. After the washing in PBS, the sections were blocked/permeabilized in blocking buffer (0.5% Tween 20, 5% donkey serum, 22.52 mg/mL glycine in PBS) for 30 min at RT in a humidified chamber. Further, sections were blocked for 1 h, at RT in blocking buffer (5% donkey serum, 22.52 mg/mL glycine in PBS), and afterwards incubated with primary antibodies overnight in blocking buffer (2% donkey serum, 22.52 mg/mL glycine in PBS) in a humidified chamber at 4 °C. After washing thrice in PBS, sections were incubated with secondary in blocking buffer (2% donkey serum, 22.52 mg/mL glycine in PBS) for 1 h at RT in a humidified chamber and then washed thrice in PBS. Nuclei were counter-stained with Hoechst 33342 solution (3 μg/mL) in PBS for 10 min in the dark. After another two washes in PBS, slides were mounted with ProLong™ Glass Antifade Mountant (Thermo Fisher Scientific). Three tumor samples per group were imaged with an LSM 800 confocal microscope (Carl Zeiss) with a 20x objective (NA 0.8). Hoechst 33342, Alexa Fluor 488, Cy3 and Alexa Fluor 647 were excited with lasers with excitation wavelengths of 405 nm, 488 nm, 561 nm and 640 nm, respectively. To capture the emitted light Gallium Arsenide Phosphide (GaAsP) detector was used combined with a variable dichroic and filters at channel specific wavelengths: 410 – 545 nm (Hoechst 33342), 488 – 545 nm (Alexa Fluor 488), 565 – 620 nm (Cy3) and 645 – 700 nm (Alexa Fluor 647). The obtained images were visualized and analyzed with Imaris software (Bitplane). Cut-off values for each channel were determined based on negative control.

2.10. Statistical analysis

For statistical analysis and graph figures GraphPad Prism 9 (GraphPad Software, CA, US) was used. Significance of expression data was determined with multiparametric *t*-test. Significance of Kaplan-Meier survival curves was determined with Log-rank test. Significance of immunofluorescence data of frozen tumor tissue sections was determined by one-way ANOVA with Dunnett's multiple comparisons post hoc test. A P-value of < 0.05 was considered to be statistically significant (* $p < 0.05$ vs control, non-treated cells or tumors (Ctrl)).

3. Results

3.1. In vitro transfection of tumor cells with plasmid DNA modifies cellular cytokine expression profile

First, the effect of lipofection with plasmid DNA encoding for either murine CCL5 or CCL17 on cell viability was determined in two murine breast cancer cell lines, 4T1 and E0771, and two murine colon cancer cell lines, CT26 and MC38. Lipofection was chosen for *in vitro* experiments due to its reported high transfection efficacy combined with low toxicity [57]. The viability of the 4T1, CT26, and MC38 cells 48 h after lipofection was above 85%, while the viability of E0771 cells was above 70% (Fig. 1A). This demonstrated that the lipofection of plasmid DNA encoding proinflammatory chemokine CCL5 or CCL17, or pDNA Ctrl – empty plasmid DNA, has low toxicity in the tumor cells and that the observed modifications of cytokine expression would not be due to cellular death. The expression of the transfected chemokines *Ccl5* and *Ccl17* was then determined on mRNA level 48 h after lipofection using qRT-PCR. Both chemokines *Ccl5* and *Ccl17* had significantly higher relative expression compared to control, non-transfected cells (Fig. 1B, C). Interestingly, among all cancer cell lines, breast cancer cell line E0771 with the lowest viability had the highest relative expression of both transgenes.

Concurrently with the expression of the transfected chemokines, the expression of nine other proinflammatory cytokines (*Cxcl9, Cxcl10, Il-1β, Il-6, Il-12α, Il-18, Ifnγ, Ifnβ* and *Tnfα*), involved in the antitumor immune response, was determined with qRT-PCR 48 h after lipofection. Interestingly, lipofection of control plasmid (pDNA Ctrl) already resulted in statistically increased expression levels of majority of the interrogated cytokines (Fig. 2A). Specifically, *Ifnβ* was upregulated in all transfected cell lines, *Il-18* and *Cxcl10* were upregulated in three cell lines, and *Cxcl9, Tnfα, Il-6*, and *Ccl5* were upregulated in two out of four cell lines (Fig. 2A). Additionally, upregulation of *Il-1β* was detected in the 4T1 cell line and upregulation of *Il-12α* in the CT26 cell line (Fig. 2A).

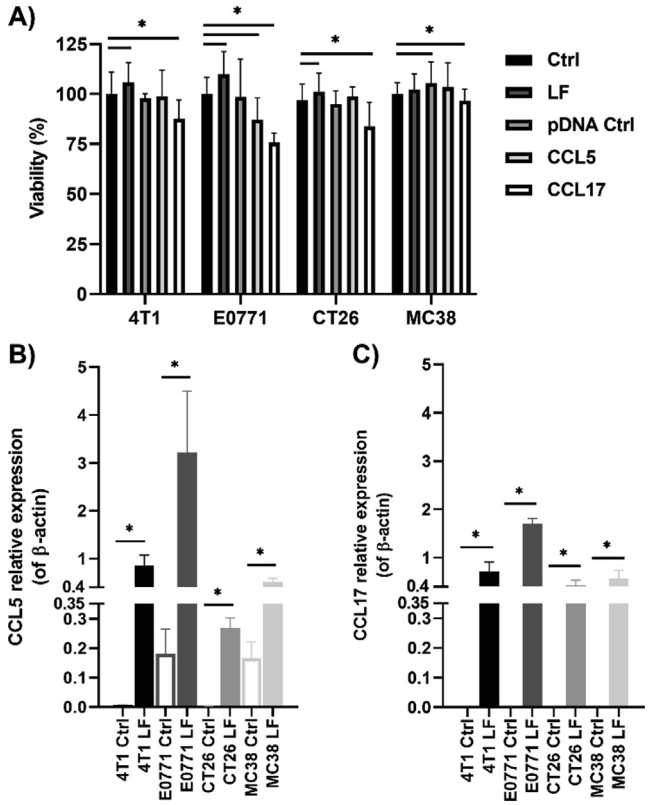

Fig. 1. Transfection efficacy and effect of lipofection with plasmid DNA encoding CCL5 or CCL17 on viability of 4T1, E0771, CT26 and MC38 cell lines. A) Viability of cells 48 h after lipofection with control plasmid DNA (pDNA Ctrl) and plasmid DNA encoding CCL5 or CCL17 determined with PrestoBlue assay. B) Relative expression of Ccl5 to β-actin after lipofection of cells with plasmid DNA encoding CCL5 and C) relative expression of Ccl17 to β-actin after lipofection of cells with plasmid DNA encoding CCL17 in 4T1, E0771, CT26 and MC38 cell lines. The expression of Ccl5 and Ccl17 in the cells was determined 48 h after lipofection with qRT-PCR. 4T1 Ctrl, E0771 Ctrl, CT26 Ctrl and MC38 Ctrl designate the expression of Ccl5 or Ccl17 in non-transfected control cells. 4T1 LF, E0771 LF, CT26 LF and MC38 LF designate the expression of Ccl5 or Ccl17 in cells transfected with plasmid DNA encoding either CCL5 or CCL17. The values are presented as AM ± SD. Statistical significance was determined by a multiparametric *t*-test. A P-value of < 0.05 was considered to be statistically significant (* $p < 0.05$ vs control, non-transfected cells).

Almost identical cytokine expression signature was determined after lipofection with plasmid DNA encoding CCL5 (Fig. 2B), with the only difference, that *Il-12α* expression was not upregulated in the CT26 cell line. A similar cytokine expression signature was also determined after lipofection with plasmid DNA encoding CCL17 with the most prominent difference in the *Ifn-β* expression, which was upregulated only in the CT26 cell line (Fig. 2C).

Taken together, the lipofection of four different tumor cell lines, 4T1, E0771, CT26, and MC38, with plasmid DNA encoding CCL5 or CCL17 is not toxic to the cells and results in a high increase in the expression of the transfected chemokines. Moreover, the cytokine expression analysis revealed that the majority of the interrogated cytokines are upregulated already after lipofection of the control plasmid DNA (pDNA Ctrl) and that neither plasmid DNA encoding CCL5 or CCL17 drastically changes this cytokine expression signature.

3.2. Gene electrotransfer of plasmid DNA encoding CCL5 or CCL17 leads to a minor tumor growth delay

The effect of CCL5 and CCL17 on tumor growth of breast cancer tumor model 4T1 and colon cancer tumor model CT26 was then determined *in vivo*. These two cell lines were chosen due to the difference in the expression of interrogated cytokines (Fig. 2B, C), because they are both syngeneic to Balb/c mice, thus eliminating the difference in the immune response due to the difference in the immune phenotype between different mouse strains and because of their different immunophenotype [58]. The CT26 tumor model is defined as immunoinflammatory due to the high infiltration of NK cells, CD4+ and CD8+ T lymphocytes, while 4T1 tumor model consists mainly of myeloid-derived suppressor cells (MDSCs), macrophages, CD4+ and Treg lymphocytes, which are responsible for its immunosuppressive phenotype [47]. For the transfection of tumors with plasmid DNA, gene electrotransfer was used, as it is a convenient and effective method for the introduction of plasmid DNA into tumors and tissues [44,59].

Both tested pulsing protocols for gene electrotransfer resulted in high expression of the enhanced green fluorescent protein (EGFP) mRNA 3 days after gene electrotransfer of plasmid DNA encoding EGFP to tumors *in vivo* (Fig. 3A). EGFP was used as a model protein, which is not naturally present in either of the two cell lines, thus allowing for direct comparison of the transfection efficiency. There was no statistically significant difference in the *Egfp* expression levels between the two pulsing protocols in either of the two tumor models as well as not between the two tumor models (Fig. 3A). When plasmid DNA encoding CCL5 was used

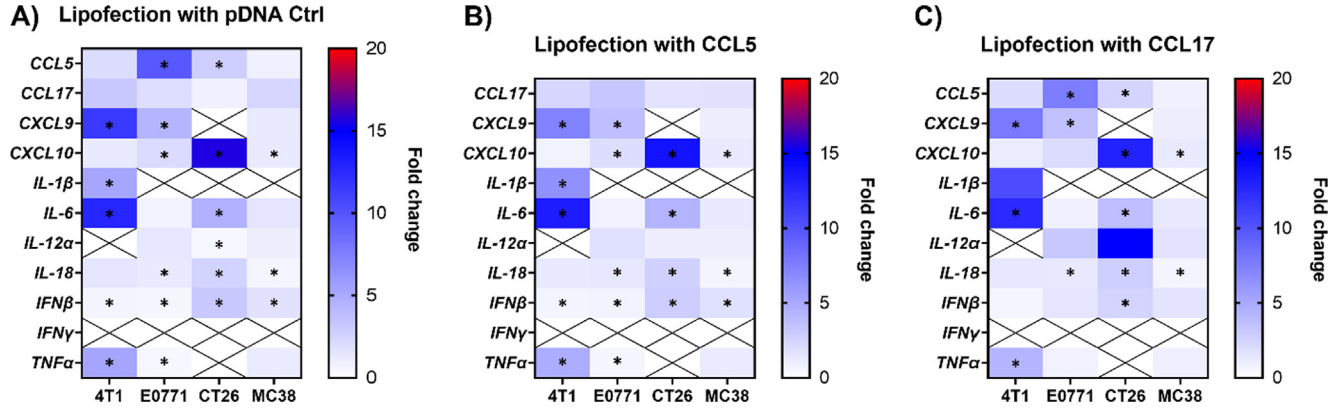

Fig. 2. Upregulation of proinflammatory cytokines after lipofection with plasmid DNA encoding CCL5 or CCL17 in 4T1, E0771, CT26 and MC38 cell lines. The expression of proinflammatory cytokines was determined 48 h after lipofection of 4T1, E0771, CT26 and MC38 cancer cells with qRT-PCR. Heat maps show increased expression, expressed as fold change relative to control, non-treated cells, of cytokines after lipofection with A) control plasmid DNA (pDNA Ctrl), B) plasmid DNA encoding CCL5, or C) plasmid DNA encoding CCL17 in 4T1, E0771, CT26 and MC38 cell lines. Crossed squares represent non-determined cytokine expression. Statistical significance was determined by a multiparametric *t*-test. A P-value of < 0.05 was considered to be statistically significant (* $p < 0.05$ vs control, non-transfected cells).

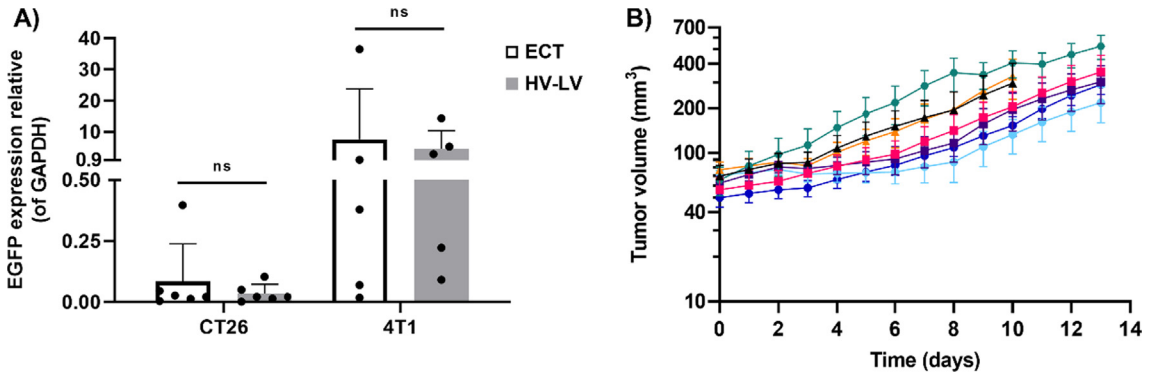

Fig. 3. Transfection efficiency and antitumor effect of GET of plasmid DNA encoding CCL5 or CCL17 using ECT or HV-LV pulsing protocol. A) The transfection efficiency in CT26 and 4T1 tumors was determined with qRT-PCR on day three after GET of plasmid DNA encoding EGFP. B) The antitumor effect of GET was evaluated by determining the tumor growth. Legend: Ctrl, pDNA Ctrl (ECT), pDNA Ctrl (HV-LV), CCL5 (ECT), CCL5 (HV-LV), CCL17 (ECT), CCL17 (HV-LV). The values are presented as AM ± SD, except in B) where AM ± SEM are presented. Statistical significance was determined by a multiparametric *t*-test. A P-value of < 0.05 was considered to be statistically significant (* $p < 0.05$ vs control, non-treated tumors (Ctrl)).

for gene electrotransfer to CT26 tumors, there was also no statistically significant difference between the two pulsing protocols in the expression levels of the *Ccl5* transgene on day three or day seven after gene electrotransfer (Fig. 4A, C). Differently, the ECT pulsing protocol, resulted in a statistically significant higher expression of *Ccl17* transgene than the HV-LV pulsing protocol, both on days three and seven, after gene electrotransfer of plasmid DNA encoding CC17 to CT26 tumors (Fig. 4A, C). Importantly, both pulsing protocols resulted in a high increase in the expression levels of the *Ccl5* and *Ccl17* transgenes in CT26 tumors (Fig. 4A, C).

To determine the effect of gene electrotransfer of plasmid DNA encoding CCL5 or CCL17 on tumor growth, the CT26 tumor model was first used. Tumor growth was followed by measuring tumor volume every two days after gene electrotransfer. Both pulsing protocols resulted in a slight, but non-statistically significant decrease in tumor growth, regardless of the plasmid used for gene electrotransfer (Fig. 3B). Similarly, the survival of mice was marginally increased after GET of pDNA Ctrl and plasmid DNA encoding CCL17, but not after GET of plasmid DNA encoding CCL5 (Fig S2).

As there was no difference in the expression of *EGFP* transgene between the different pulsing protocols in CT26 and in 4T1 tumor model (Fig. 3A), the ECT pulsing protocol resulted in a higher expression of *Ccl17* transgene in the CT26 tumor model (Fig. 4A, C), and there was no difference in tumor growth after gene electrotransfer between the two pulsing protocols (Fig. 3B), only the ECT pulsing protocol was further used in 4T1 tumor model. Expectedly, gene electrotransfer of plasmid DNA encoding CCL5 or CCL17 to 4T1 tumors using the ECT pulsing protocol resulted in a high expression levels of both transgenes three and seven days after gene electrotransfer (Fig. 4B, D). Similarly as in the CT26 tumor model (Fig. 3B, 5A), gene electrotransfer of plasmid DNA encoding CCL5 or CCL17 to 4T1 tumors resulted in a slight, but non-statistically significant decrease in tumor growth (Fig. 5B). The calculated tumor growth delay (Fig. 5C) showed that the 4T1 tumors were even less responsive than the CT26 tumors to the GET of plasmid DNA encoding CCL5 or CCL17 as well as to the control plasmid pDNA Ctrl. This was recapitulated also in the survival of mice, as GET of plasmid DNA encoding CCL17 and pDNA Ctrl significantly prolonged the survival of mice in the CT26 tumor model

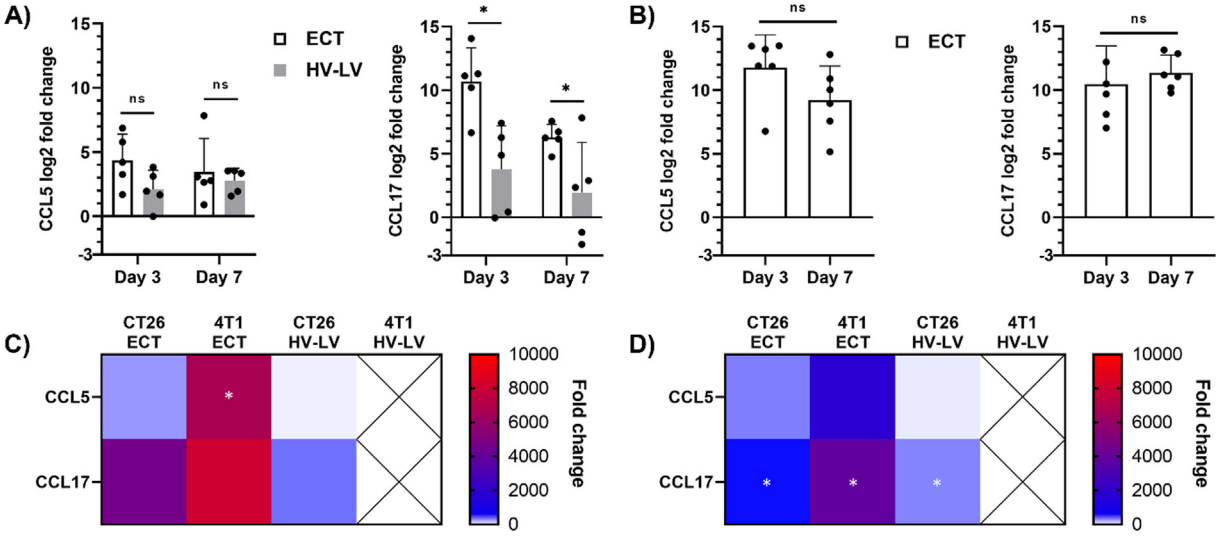

Fig. 4. Upregulation of chemokines CCL5 and CCL17 after GET of plasmid DNA encoding CCL5 or CCL17 in CT26 and 4T1 tumors using ECT or HV-LV pulsing protocol. Expression of Ccl5 and Ccl17 in A) CT26 and B) 4T1 tumors was determined with qRT-PCR on days three and seven after GET of plasmid DNA encoding CCL5 or CCL17. Heat maps show increased expression, expressed as fold change relative to control, non-treated cells, of CCL5 and CCL17 in CT26 and 4T1 tumors on C) day three and D) day seven after GET of plasmid DNA encoding CCL5 or CCL17. Crossed squares represent unperformed GET. The values are presented as AM ± SD. Statistical significance was determined by a multiparametric *t*-test. A P-value of < 0.05 was considered to be statistically significant (* $p < 0.05$ vs control, non-treated tumors (Ctrl)).

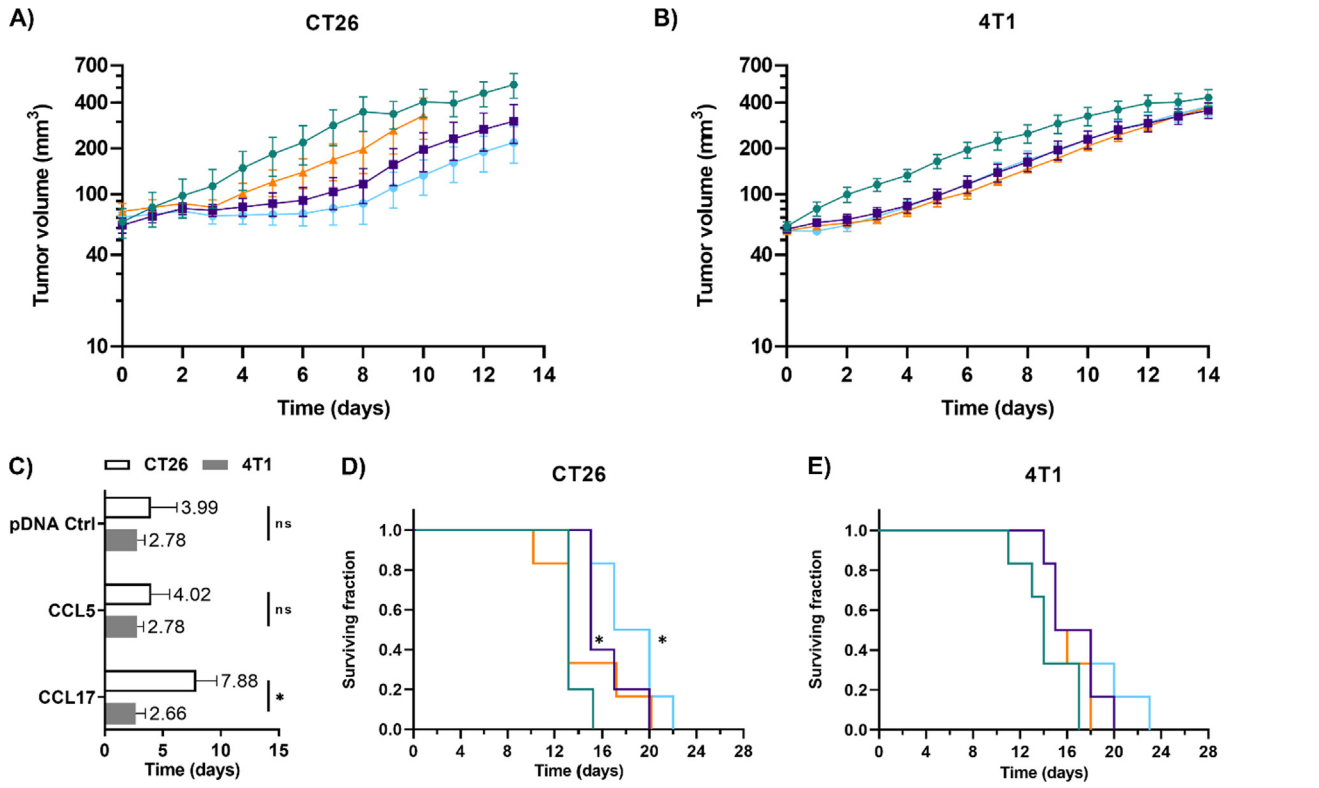

Fig. 5. Survival of mice after GET of plasmid DNA encoding CCL5 or CCL17 into CT26 and 4T1 tumors. Tumor growth after GET of control plasmid DNA (pDNA Ctrl) and plasmid DNA encoding CCL5 or CCL17 using ECT pulses was determined for A) CT26 and B) 4T1 tumors. Legend: Ctrl, pDNA Ctrl, CCL5, CCL17. C) Growth delay of CT26 and 4T1 tumors after treatment was calculated using tumor doubling time. Kaplan–Meier (KM) curves show the overall survival of mice after the treatment of D) CT26 and E) 4T1 tumors. Legend: Ctrl, pDNA Ctrl, CCL5, CCL17. The values in A, B and C are presented as AM ± SEM. Statistical significance was determined by a multiparametric *t*-test. A P-value of < 0.05 was considered to be statistically significant (* $p < 0.05$ vs control, non-treated tumors (Ctrl)). Statistical significance of KM curves was determined by the Log-rank test. A P-value of < 0.05 was considered to be statistically significant (* $p < 0.05$ vs control, non-treated tumors (Ctrl)).

(Fig. 5D), whereas this was not the case in the 4T1 tumor model (Fig. 5E).

Thus, despite achieving high levels of *Ccl5* and *Ccl17* transgene expression in both tumor models, regardless of the pulsing protocol used, GET of plasmid DNA encoding CCL5 or CCL17 has only a minor effect on tumor growth and the survival of mice.

3.3. GET of plasmid DNA encoding CCL5 or CCL17 modifies cytokine expression in CT26 tumors

In order to determine whether GET of plasmid DNA encoding CCL5 or CCL17 can modify the immune infiltrate of the tumor microenvironment, the expression of a subset of cytokines from the *in vitro* experiments was determined with qRT-PCR three and seven days after GET in both tumor models. Based on the *in vitro* results (Fig. 2) the cytokines CXCL9, CXCL10, IL-6, IL-12α, and IFNγ were chosen.

In the CT26 tumor model, both pulsing protocols were used. The ECT pulsing protocol resulted in an increased expression of *Il-6* three days after GET of either of the plasmids, but it was statistically significant only when pDNA Ctrl was used (Fig. 6A). Differently, seven days after GET, *Ifnγ* and *Cxcl9* were most prominently expressed when plasmid DNA encoding CCL5 or CCL17 were used (Fig. 6B). The increased expression of *Cxcl10*, *Il-6*, and *Il-12α* seven days after GET was only determined when plasmid DNA encoding CCL5 was used (Fig. 6B). Similarly, the use of HV-LV pulsing protocol resulted in an increased expression of *Il-6* three days after GET (Fig. 6C), whereas, only *Cxcl10* and *Ifnγ* were upregulated seven days after GET of plasmid DNA encoding CCL5 (Fig. 6D), indicating a smaller effect of this pulsing protocol on the immune infiltrate in the CT26 tumor microenvironment. In the case of 4T1 tumor model, only ECT pulsing protocol was used, and as was the case in the *in vitro* experiments (Fig. 2), the detected changes in cytokine expression were less prominent than in the CT26 tumor model (Fig. 6E, F). Although the increase in expression of all five cytokines was determined, it was not statistically significant neither three days (Fig. 6E) nor seven days (Fig. 6F) after GET.

3.4. GET of plasmid DNA encoding CCL5 or CCL17 modifies immune cell populations in the tumor microenvironment

The presence of inflammatory cytokines in the tumor microenvironment may lead to the infiltration of different immune cells into the tumor [9]. Thus, to determine if GET of plasmid DNA encoding CCL5 or CCL17 leads to the infiltration of immune cells, frozen sections of tumors taken three or seven days after GET were immunofluorescently stained for CD8+ T lymphocytes, CD4+ helper T lymphocytes, macrophages (F4/80 surface expression) and blood vessels (CD31 expression).

The presence of all three interrogated immune cell populations was confirmed in both tumor models with the CT26 tumor having more CD8+ than CD4+ cells (Fig. 7, Figs S3, S6A-C), whereas the 4T1 tumors had more CD4+ than CD8+ cells (Fig. 8, Figs S5, S6G-I), which is in line with the published literature [47]. The F4/80 positive area indicating the presence of macrophages was mostly observed in the tumor edge in both tumor models (Figs. 7, 8, Figs

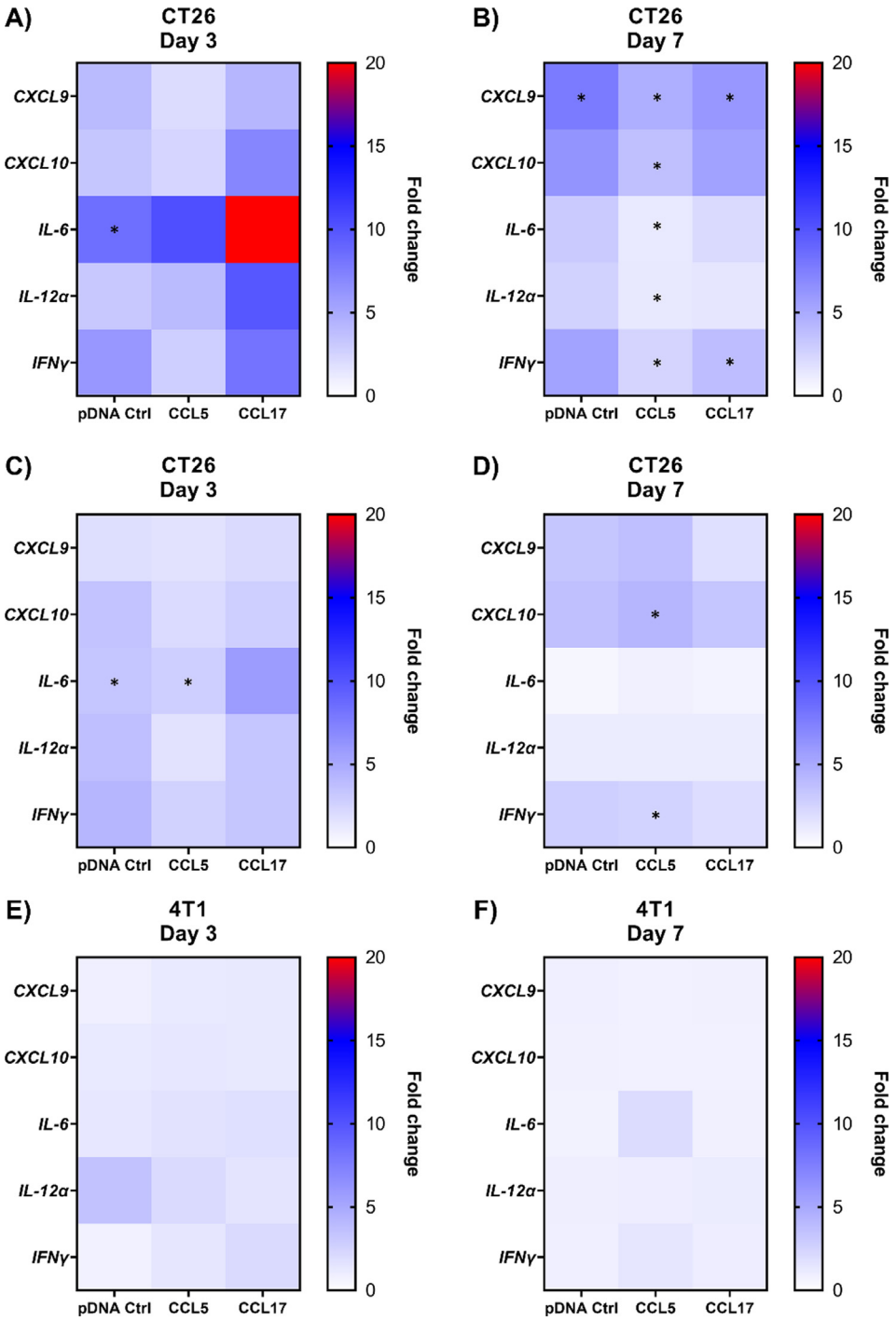

Fig. 6. Upregulation of proinflammatory cytokines after GET of plasmid DNA encoding CCL5 or CCL17 in CT26 and 4T1 tumors. Heat maps show increased expression, expressed as fold change relative to control, non-treated cells, of proinflammatory cytokines in tumors determined with qRT-PCR on days three and seven after GET of control plasmid DNA (pDNA Ctrl) and plasmid DNA encoding CCL5 or CCL17. Heat maps show increased expression of proinflammatory cytokines in CT26 tumors after GET using A, B) ECT pulses and C, D) HV-LV pulses, while heat maps E, F) show increased expression of proinflammatory cytokines in 4T1 tumors after GET using ECT pulses. Statistical significance was determined by a multiparametric *t*-test. A P-value of < 0.05 was considered to be statistically significant (* $p < 0.05$ vs control, non-treated tumors (Ctrl)).

S3, S5). Both tumor models had similar vascularization as the percent of blood vessel area was between 5.20% and 5.99% (Fig S6D, J).

Contrary to the expected role of CCL5 and CCL17 as a chemoattractant for immune cells [10], GET of plasmid DNA encoding CCL5 or CCL17, or pDNA Ctrl did not significantly modify the interrogated populations of immune cells. Specifically, GET with either the ECT pulsing protocol or HV-LV pulsing protocol did not statistically significantly change the number of CD4+ (Fig. 7, Figs S3, S4, S6A, S7A) or CD8+ (Fig. 7, Figs S3, S4, S6B, S7B) cells in the tumor, nor their distance from blood vessels (Figs S6D, E, S7D, E) three or seven days after GET in the CT26 tumor model. Similarly, the presence of macrophages remained unaffected (Fig. 7, Figs S3, S4). This was also recapitulated in the 4T1 tumor model, where GET of plasmid DNA encoding CCL5 or CCL17 or pDNA Ctrl, using the ECT pulsing protocol also did not statistically significantly change the number of CD4+ (Fig. 8, Figs S5, S6G) or CD8+ (Fig. 8, Figs S5,

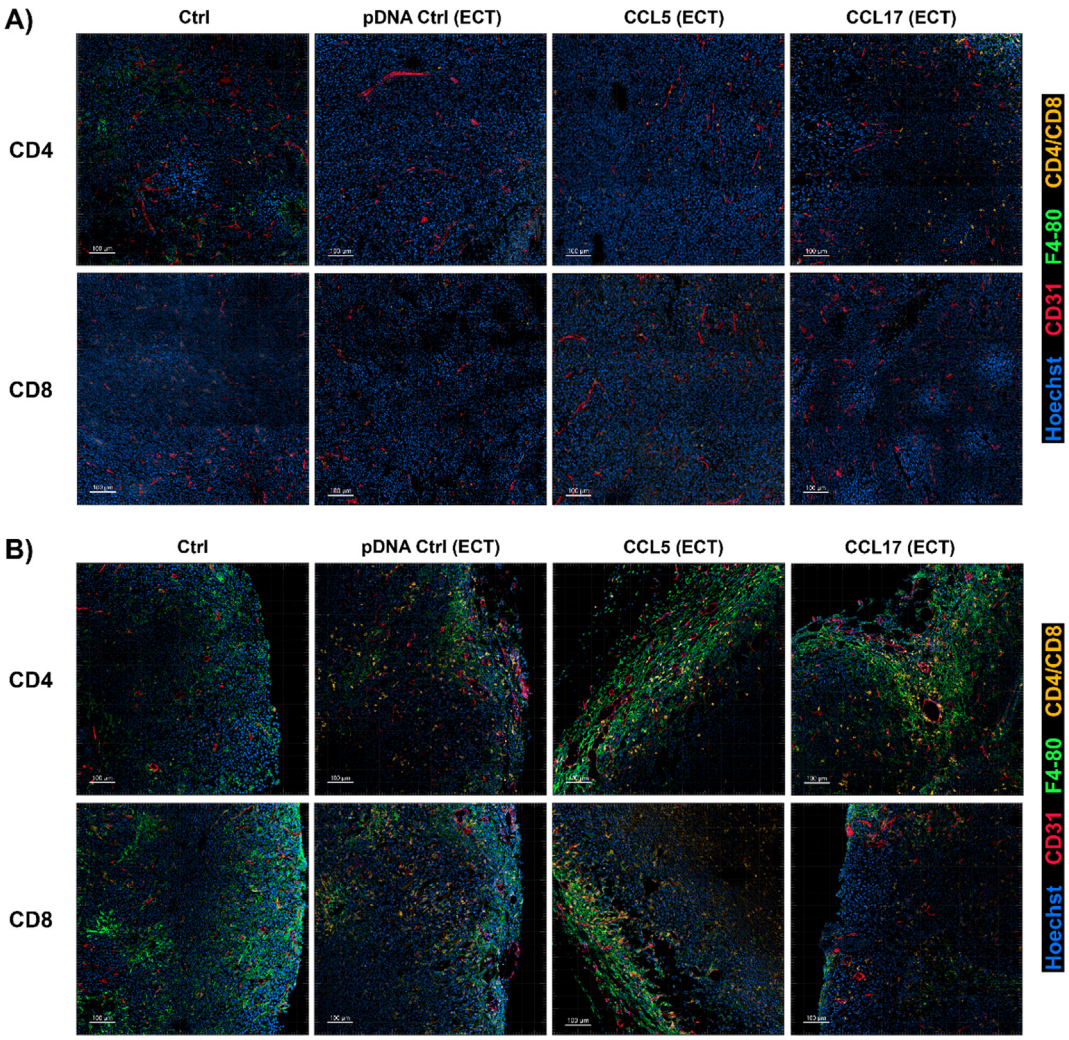

Fig. 7. GET of plasmid DNA encoding CCL5 or CCL17 to CT26 tumors impacts immune cell infiltration to tumor tissue. GET was performed using ECT pulses. Tumors were collected on day seven after GET for histological analysis. Frozen sections of tumor tissue were stained with anti-CD4 or anti-CD8 (yellow, Cy3), anti-CD31 (red, Alexa 647), anti-F4/80 (green, Alexa 488) and Hoechst 33342 (blue). The representative images of A) tumor center and B) tumor edge are shown. Yellow: Cy3; Red: Alexa 647; Green: Alexa 488; Blue: Hoechst 33342. Scale bar: 100 μm. (For interpretation to colours in this figure, the reader is referred to the web version of this paper.)

S6H) cells in the tumor, nor their distance from blood vessels (Fig S6J, K). As in the CT26 tumor model the presence of macrophages remained unaffected (Fig. 8, Fig S5).

Thus, despite the expected chemoattractive properties of the expressed *Ccl5* and *Ccl17* transgenes (Fig. 4A-D) and modified expression of several other proinflammatory cytokines (Fig. 6) there was no change in the interrogated populations of immune cells after GET of plasmid DNA encoding CCL5 or CCL17 in either CT26 or 4T1 tumor model.

4. Discussion

In this study, we demonstrated that *in vitro* lipofection of plasmid DNA encoding proinflammatory chemokines CCL5 and CCL17 results in a high expression of both transgenes in four cancer cell lines, two murine breast cell lines, 4T1 and E0771, and two colon cancer cell lines, CT26 and MC38, with a concomitant substantial upregulation of several other proinflammatory cytokines. Interestingly, the same subset of proinflammatory chemokines was also upregulated when control plasmid DNA was used. Further, we have demonstrated that when gene electrotransfer (GET) is used for the delivery of plasmid DNA encoding CCL5 or CCL17 to CT26 and 4T1 tumors *in vivo*, high transgene expression levels can be achieved using the standard electric pulsing protocol used for electrochemotherapy (ECT) in clinics [50]. These high transgene expression levels, however, did not translate into a pronounced anti-tumor effect, but only slightly prolonged the survival of the treated mice. Moreover, after GET with either of the plasmids we only detected minor changes in the expression of other proinflammatory chemokines *in vivo*, as well as non-significant changes in the populations of CD4+ helper T lymphocytes, CD8+ T lymphocytes, F4/80 macrophages and in the presence of blood vessels.

Although GET is a highly efficient and convenient method for local plasmid DNA delivery to different tumors and tissues *in vivo* [44], there are several drawbacks to using it *in vitro*. GET *in vitro* has a known variability in transfection efficiency and cell viability between different cell lines and pulsing protocols [60,61]. Moreover, electric pulses alone, including the ECT pulsing protocol used in this study *in vivo*, can already influence the expression levels of several genes [62]. Furthermore, often the optimal gene electrotransfer parameters determined in 2D cell culture *in vitro* are not recapitulated even in 3D cell cultures and even less often *in vivo* [61,63,64]. Thus, we have decided to use lipofection for the *in vitro* experiments, which is less toxic for the cells and has lower variability in the transfection efficiency between

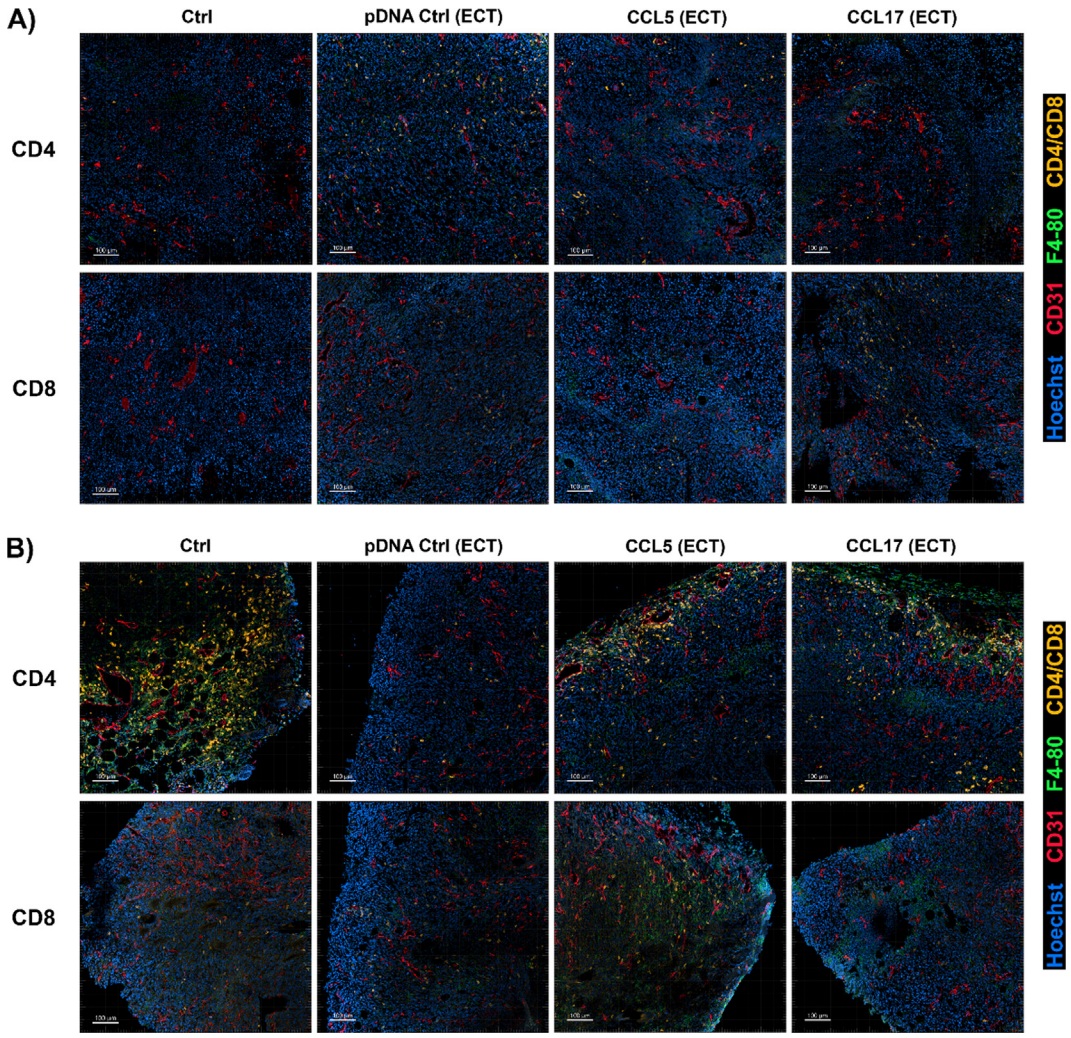

Fig. 8. GET of plasmid DNA encoding CCL5 or CCL17 to 4T1 tumors impacts immune cell infiltration to tumor tissue. GET was performed using ECT pulses. Tumors were collected on day seven after GET for histological analysis. Frozen sections of tumor tissue were stained with anti-CD4 or anti-CD8 (yellow, Cy3), anti-CD31 (red, Alexa 647), anti-F4/80 (green, Alexa 488) and Hoechst 33342 (blue). The representative images of A) tumor center and B) tumor edge are shown. Yellow: Cy3; Red: Alexa 647; Green: Alexa 488; Blue: Hoechst 33342. Scale bar: 100 μm. (For interpretation to colours in this figure, the reader is referred to the web version of this paper.)

different cell lines [57]. Using this approach, it was demonstrated that a high *Ccl5* or *Ccl17* transgene expression levels in all four cell lines is not more cytotoxic than the lipofectamine alone or lipofection of empty control plasmid DNA. Moreover, the majority of the determined changes in the expression of the interrogated proinflammatory cytokines were common to all three plasmid DNAs used, including the control plasmid DNA, in all four cell lines. This implies that the observed changes in the cytokine expression are due to the entry of foreign plasmid DNA into the cell's cytosol and not due to the expression of either of the transgenes. Indeed, increased expression of several cytokines, among them *Il-1β*, *Ifnβ*, *Il-18*, *Tnfα*, *Il-6*, *Ccl5*, *Cxcl9*, *Cxcl10* is often observed upon the activation of cytosolic DNA sensors or the cyclic GMP-AMP synthase (*cGas*) – Stimulator of interferon genes (*Sting*) (*cGas-Sting*) pathway regardless of the method used for the delivery of foreign DNA into the cells [65-69].

In the *in vivo* setting, the comparison of two different electric pulsing protocols confirmed that both ECT and HV-LV pulsing protocols, can achieve high levels of transgene expression in the CT26 and in the 4T1 tumor model tumor that lasts for at least seven days after GET. For the majority of tissues including skin and muscle pulse application is recommended and performed immediately after the plasmid injection [70,71]. However, our group has found that a 5 min delay between the injection of plasmid DNA and delivery of electric pulses, works best when tumors are the target tissue [72]. Following the published literature on the evaluation of electroporation and gene electrotransfer efficacy [73], we have first evaluated *in vivo* the two electro pulsing protocols used in the study by performing gene electrotransfer of plasmid DNA encoding enhanced green fluorescent protein (EGFP), thus providing a direct comparison of gene electrotransfer efficacy between both pulsing protocols and both tumor models. In this study, we did not detect differences in the gene electrotransfer efficacy between the two tumor models or the two pulsing protocols used as determined by qRT-PCR of EGFP expression (Fig. 3A), thus we believe we can attribute the observed differences in the response of tumors to gene electrotransfer of plasmid DNA encoding CCL5 or CCL17 to the different tumor immune phenotype, rather to the differences in gene electrotransfer efficacy. This is in line with the published literature and ongoing clinical trials with the intratumoral gene electrotransfer of plasmid IL-12 (tavokinogene telseplasmid; "tavo") where a similar pulsing protocol is used, with the only difference being that it comprises of six pulses instead of eight, as was the case in our study [53,74]. The majority of electric pulsing protocols used for GET use so-called long pulses, whose duration is in the order of several milliseconds [75]. Although a high transgene

expression levels, and a good therapeutic efficacy can be achieved with these pulsing protocols, their drawback comes in a form of a pronounced anti-tumor effect, even when control plasmid DNA or even single- or double-stranded DNA is used [76]. Contrary, the ECT pulsing protocol used in our study resulted only in a minor anti-tumor effect in both the CT26 and 4T1 tumor models when control plasmid DNA was used for GET. This raises the possibility for more precise studies of the effects of the introduced transgenes unencumbered by the effects caused by the electric pulses alone.

The increased expression of the transgenes was accompanied by an increase in the expression levels of several proinflammatory cytokines. This increase was tumor model, plasmid DNA, and electro pulsing protocol specific. Whereas there was no change in the cytokine expression levels after GET in the 4T1 tumor model, several cytokines were upregulated in the CT26 tumor model. When using the ECT pulsing protocol the upregulation of *Cxcl9*, *Cxcl10*, *Ifnγ*, *Il-12α*, and *Il-6* expression was determined seven days after GET of plasmid DNA encoding CCL5, as was the upregulation of *Cxcl9* and *Ifnγ* expression after GET of plasmid DNA encoding CCL17. On the other hand, the only cytokine with upregulated expression three days after GET was *Il-6*. Changes in the expression levels of *Il-6*, *Cxcl10* and *Ifnγ* were also observed when HV-LV pulsing protocol was used for GET in the CT26 tumor model. Increased expression of *Cxcl10* and *Cxcl9* has been correlated with the presence of tumor infiltrating T lymphocytes, activation of Th1 cells within TME and favorable response to immunotherapies [15,77]. In addition, both CXCL9 and CXCL10 are potent inhibitors of angiogenesis [78]. Moreover, epigenetic studies showed that *Cxcl10*, *Cxcl9* and *Ccl5* are epigenetically silenced in immunosuppressive tumors such as 4T1 [79,80]. Thus, reviving the expression of epigenetically silenced *Cxcl10*, *Cxcl9* or *Ccl5* could improve the Th1 cell activation and infiltration of effector immune cells. Similarly, IL-12α promotes the development of Th1 responses, increases the activation and cytotoxic capacities of T lymphocytes and NK cells, inhibits or reprograms immunosuppressive cells and induces the production of large amounts of IFNγ [44,81,82]. Further, IFNγ, a product of Th1-mediated immune response, coordinates Th1 effector mechanisms, and further activates the macrophages and NK cells in a positive feedback loop [83]. Taken together, the upregulated expression of these cytokines after GET could divert the TME towards the Th1 response and tumor regression. On the other hand, the increased expression of *Il-6* after GET, which regulates the main hallmarks of cancer and multiple signaling pathways, including apoptosis, survival, proliferation, angiogenesis, invasiveness, metastasis and metabolism [84,85], could divert the TME towards the Th2 response, thus hampering the anti-tumor effects.

In our study, the close examination of the TME by immunofluorescence staining of CD4+ helper T lymphocytes, CD8+ T lymphocytes, F4/80 macrophages, and blood vessels did not determine any significant modifications of the TME composition in the CT26 or 4T1 tumor model. This implies either that other immune cell populations are affected, such as NK cells, MDSCs, or that the increased expression of *Il-6* can abrogate the effects of other cytokines that were upregulated and should drive the TME towards the Th1 response.

A limitation of our study was that only a single and not repetitive GET was tested. It was already demonstrated that repetitive GET of plasmid DNAs is more effective than a single GET [86]. One important factor that should be taken into account in the future is that immunotherapies are predominantly used as adjuvant therapies to chemotherapy or radiotherapy [87]. Thus, an optimized GET dosing regimen in combination with a standard cancer therapy could still hold promise for the exploitation of proinflammatory chemokines such as CCL5 and CCL17 for cancer immunotherapy.

5. Conclusions

To summarize, this study demonstrates that high levels of *Ccl5* or *Ccl17* transgene expression can be achieved *in vitro* with lipofection in four different cancer cell lines and that the resulting change in the cytokine expression is due to the introduction of plasmid DNA into the cells and not the transgene expression. *In vivo* this study confirms that ECT pulsing protocol achieves high levels of transgene expression in the tumors with a minimal anti-tumor effect when control plasmid DNA is used. Although a minor prolongation in mice survival was confirmed after GET of plasmid DNA encoding CCL5 or CCL17, and an upregulation of several proinflammatory cytokines was determined, this had no effect on the composition of TME. Optimizing the GET dosing regimen, especially if combined with a standard cancer therapy, could still position the proinflammatory chemokines such as CCL5 and CCL17 among potential novel cancer immunotherapies.

Author contributions

Conceptualization: M.C. G.S., B.M.; Methodology, data acquisition and analysis: T.B., M.C., S.K. and B.M.; Writing: T. B., M.C., B. M.; Review and editing: B.M., M.C., and G.S.; All authors have read and agreed to the published version of the manuscript.

Declaration of Competing Interest

The authors declare that they have no known competing financial interests or personal relationships that could have appeared to influence the work reported in this paper.

Acknowledgments

This work was supported by the Slovenian Research Agency (ARRS), grant number J3-8202 and P3-0003.The investment was co-financed by The Republic of Slovenia and The European Regional Development Fund within the scope of SmartGene.Si. We would like to thank Mira Lavric (Institute of Oncology Ljubljana, Ljubljana, Slovenia) for her technical help.

Appendix A. Supplementary data

Supplementary data to this article can be found online at https://doi.org/10.1016/j.bioelechem.2021.107795.

References

[1] S.T. Paijens, A. Vledder, M. de Bruyn, H.W. Nijman, Tumor-infiltrating lymphocytes in the immunotherapy era, Cell. Mol. Immunol. (2020) 1–18, https://doi.org/10.1038/s41423-020-00565-9.
[2] R.R. Weichselbaum, H. Liang, L. Deng, Y.X. Fu, Radiotherapy and immunotherapy: A beneficial liaison?, Nat. Rev. Clin. Oncol. 14 (2017) 365–379, https://doi.org/10.1038/nrclinonc.2016.211.
[3] L. Galluzzi, T.A. Chan, G. Kroemer, J.D. Wolchok, A. López-Soto, The hallmarks of successful anticancer immunotherapy, Sci. Transl. Med. 10 (2018) 1–15, https://doi.org/10.1126/scitranslmed.aat7807.
[4] D. Bruni, H.K. Angell, J. Galon, The immune contexture and Immunoscore in cancer prognosis and therapeutic efficacy, Nat. Rev. Cancer. 20 (2020), https://doi.org/10.1038/s41568-020-0285-7.
[5] Q. Duan, H. Zhang, J. Zheng, L. Zhang, Turning Cold into Hot: Firing up the Tumor Microenvironment, Trends in Cancer. 6 (2020) 605–618, https://doi.org/10.1016/j.trecan.2020.02.022.
[6] C. Robert, A decade of immune-checkpoint inhibitors in cancer therapy, Nat. Commun. 11 (2020) 10–12, https://doi.org/10.1038/s41467-020-17670-y.
[7] M.T. Chow, A.D. Luster, Chemokines in Cancer Melvyn, Cancer Immunol. Res. 2 (2014) 1125–1131, https://doi.org/10.1158/2326-6066.CIR-14-0160.Chemokines.
[8] K. Chen, Z. Bao, P. Tang, W. Gong, T. Yoshimura, J.M. Wang, Chemokines in homeostasis and diseases, Cell. Mol. Immunol. 15 (2018) 324–334, https://doi.org/10.1038/cmi.2017.134.

[9] R.M. Ransohoff, Chemokines and Chemokine Receptors: Standing at the Crossroads of Immunobiology and Neurobiology, Immunity. 31 (2009) 711–721, https://doi.org/10.1016/j.immuni.2009.09.010.
[10] N. Nagarsheth, M.S. Wicha, W. Zou, Chemokines in the cancer microenvironment and their relevance in cancer immunotherapy, Nat. Rev. Immunol. 17 (2017) 559–572, https://doi.org/10.1038/nri.2017.49.
[11] E. Lavergne, C. Combadière, M. Iga, A. Boissonnas, O. Bonduelle, M. Maho, P. Debré, B. Combadiere, Intratumoral CC Chemokine Ligand 5 Overexpression Delays Tumor Growth and Increases Tumor Cell Infiltration, J. Immunol. 173 (2004) 3755–3762, https://doi.org/10.4049/jimmunol.173.6.3755.
[12] C. Esche, C. Stellato, L.A. Beck, Chemokines: Key players in innate and adaptive immunity, J. Invest. Dermatol. 125 (2005) 615–628, https://doi.org/10.1111/j.0022-202X.2005.23841.x.
[13] O. Chan, J.D. Burke, D.F. Gao, E.N. Fish, The chemokine CCL5 regulates glucose uptake and AMP kinase signaling in activated T cells to facilitate chemotaxis, J. Biol. Chem. 287 (2012) 29406–29416, https://doi.org/10.1074/jbc.M112.348946.
[14] G. An, F. Wu, S. Huang, L. Feng, J. Bai, S. Gu, X. Zhao, Effects of CCL5 on the biological behavior of breast cancer and the mechanisms of its interaction with tumor-associated macrophages, Oncol. Rep. 42 (2019) 2499–2511, https://doi.org/10.3892/or.2019.7344.
[15] D. Dangaj, M. Bruand, A.J. Grimm, C. Ronet, D. Barras, P.A. Duttagupta, E. Lanitis, J. Duraiswamy, J.L. Tanyi, F. Benencia, J. Conejo-Garcia, H.R. Ramay, K.T. Montone, D.J. Powell, P.A. Gimotty, A. Facciabene, D.G. Jackson, J.S. Weber, S.J. Rodig, S.F. Hodi, L.E. Kandalaft, M. Irving, L. Zhang, P. Foukas, S. Rusakiewicz, M. Delorenzi, G. Coukos, Cooperation between Constitutive and Inducible Chemokines Enables T Cell Engraftment and Immune Attack in Solid Tumors, Cancer Cell. 35 (2019) 885–900.e10, https://doi.org/10.1016/j.ccell.2019.05.004.
[16] A. González-Martín, L. Gómez, J. Lustgarten, E. Mira, S. Mañes, Maximal T cell-mediated antitumor responses rely upon CCR5 expression in both CD4+ and CD8+ T cells, Cancer Res. 71 (2011) 5455–5466, https://doi.org/10.1158/0008-5472.CAN-11-1687.
[17] J.P. Böttcher, E. Bonavita, P. Chakravarty, H. Blees, M. Cabeza-Cabrerizo, S. Sammicheli, N.C. Rogers, E. Sahai, S. Zelenay, C. Reis e Sousa,, NK Cells Stimulate Recruitment of cDC1 into the Tumor Microenvironment Promoting Cancer Immune Control, Cell. 172 (2018) 1022–1037.e14, https://doi.org/10.1016/j.cell.2018.01.004.
[18] O. Melaiu, M. Chierici, V. Lucarini, G. Jurman, L.A. Conti, R. De Vito, R. Boldrini, L. Cifaldi, A. Castellano, C. Furlanello, V. Barnaba, F. Locatelli, D. Fruci, Cellular and gene signatures of tumor-infiltrating dendritic cells and natural-killer cells predict prognosis of neuroblastoma, Nat. Commun. 11 (2020) 1–15, https://doi.org/10.1038/s41467-020-19781-y.
[19] J.M. Araujo, A.C. Gomez, A. Aguilar, R. Salgado, J.M. Balko, L. Bravo, F. Doimi, D. Bretel, Z. Morante, C. Flores, H.L. Gomez, J.A. Pinto, Effect of CCL5 expression in the recruitment of immune cells in triple negative breast cancer, Sci. Rep. 8 (2018) 1–9, https://doi.org/10.1038/s41598-018-23099-7.
[20] M.K. Kranjc, M. Novak, R.G. Pestell, T.T. Lah, Cytokine CCL5 and receptor CCR5 axis in glioblastoma multiforme, Radiol. Oncol. 53 (2019) 397–406, https://doi.org/10.2478/raon-2019-0057.
[21] S. Trellakis, K. Bruderek, C.A. Dumitru, H. Gholaman, X. Gu, A. Bankfalvi, A. Scherag, J. Hütte, N. Dominas, G.F. Lehnerdt, T.K. Hoffmann, S. Lang, S. Brandau, Polymorphonuclear granulocytes in human head and neck cancer: Enhanced inflammatory activity, modulation by cancer cells and expansion in advanced disease, Int. J. Cancer. 129 (2011) 2183–2193, https://doi.org/10.1002/ijc.25892.
[22] N.M. Kaskas, T. Moore-Medlin, G.B. McClure, O. Ekshyyan, J.A. Vanchiere, C.A.O. Nathan, Serum biomarkers in head and neck squamous cell cancer, JAMA Otolaryngol. - Head Neck Surg. 140 (2014) 5–11, https://doi.org/10.1001/jamaoto.2013.5688.
[23] M. Sadeghi, I. Lahdou, H. Oweira, V. Daniel, P. Terness, J. Schmidt, K.H. Weiss, T. Longerich, P. Schemmer, G. Opelz, A. Mehrabi, Serum levels of chemokines CCL4 and CCL5 in cirrhotic patients indicate the presence of hepatocellular carcinoma, Br. J. Cancer. 113 (2015) 756–762, https://doi.org/10.1038/bjc.2015.227.
[24] E.J. Duell, D.P. Casella, R.D. Burk, K.T. Kelsey, E.A. Holly, Inflammation, genetic polymorphisms in proinflammatory genes TNF-A, RANTES, and CCR5, and risk of pancreatic adenocarcinoma, Cancer Epidemiol. Biomarkers Prev. 15 (2006) 726–731, https://doi.org/10.1158/1055-9965.EPI-05-0797.
[25] G.G. Vaday, D.M. Peehl, P.A. Kadam, D.M. Lawrence, Expression of CCL5 (RANTES) and CCR5 in prostate cancer, Prostate. 66 (2006) 124–134, https://doi.org/10.1002/pros.20306.
[26] R. Huang, S. Wang, N. Wang, Y. Zheng, J. Zhou, B. Yang, X. Wang, J. Zhang, L. Guo, S. Wang, Z. Chen, Z. Wang, S. Xiang, CCL5 derived from tumor-associated macrophages promotes prostate cancer stem cells and metastasis via activating β-catenin/STAT3 signaling, Cell Death Dis. 11 (2020), https://doi.org/10.1038/s41419-020-2435-y.
[27] J. Wang, Y. Wang, F. Kong, R. Han, W. Song, D. Chen, L. Bu, S. Wang, J. Yue, L. Ma, Identification of a six-gene prognostic signature for oral squamous cell carcinoma, J. Cell. Physiol. 235 (2020) 3056–3068, https://doi.org/10.1002/jcp.29210.
[28] Y. Fujimoto, N. Inoue, K. Morimoto, T. Watanabe, S. Hirota, M. Imamura, Y. Matsushita, T. Katagiri, H. Okamura, Y. Miyoshi, Significant association between high serum CCL5 levels and better disease-free survival of patients with early breast cancer, Cancer Sci. 111 (2020) 209–218, https://doi.org/10.1111/cas.14234.
[29] N. Lapteva, X.F. Huang, CCL5 as an adjuvant for cancer immunotherapy, Expert Opin. Biol. Ther. 10 (2010) 725–733, https://doi.org/10.1517/14712591003657128.
[30] T. Imai, M. Baba, M. Nishimura, M. Kakizaki, S. Takagi, O. Yoshie, The T cell-directed CC chemokine TARC is a highly specific biological ligand for CC chemokine receptor 4, J. Biol. Chem. 272 (1997) 15036–15042, https://doi.org/10.1074/jbc.272.23.15036.
[31] S. Santulli-Marotto, K. Boakye, E. Lacy, S.J. Wu, J. Luongo, K. Kavalkovich, A. Coelho, C.M. Hogaboam, M. Ryan, Engagement of two distinct binding domains on CCL17 is required for signaling through CCR4 and establishment of localized inflammatory conditions in the lung, PLoS One. 8 (2013), https://doi.org/10.1371/journal.pone.0081465.
[32] S. Scheu, S. Ali, C. Ruland, V. Arolt, J. Alferink, The C-C chemokines CCL17 and CCL22 and their receptor CCR4 in CNS autoimmunity, Int. J. Mol. Sci. 18 (2017), https://doi.org/10.3390/ijms18112306.
[33] V. Semmling, V. Lukacs-Kornek, C.A. Thaiss, T. Quast, K. Hochheiser, U. Panzer, J. Rossjohn, P. Perlmutter, J. Cao, D.I. Godfrey, P.B. Savage, P.A. Knolle, W. Kolanus, I. Förster, C. Kurts, Alternative cross-priming through CCL17-CCR4-mediated attraction of CTLs toward NKT cell-licensed DCs, Nat. Immunol. 11 (2010) 313–320, https://doi.org/10.1038/ni.1848.
[34] P. Bousso, M.L. Albert, Signal 0 for guided priming of CTLs: NKT cells do it too, Nat. Immunol. 11 (2010) 284–286, https://doi.org/10.1038/ni0410-284.
[35] M. Valente, Y. Dölen, E. van Dinther, L. Vimeux, M. Fallet, V. Feuillet, C.G. Figdor, Cross-talk between iNKT cells and CD8 T cells in the spleen requires the IL-4/CCL17 axis for the generation of short-lived effector cells, Proc. Natl. Acad. Sci. U. S. A. 116 (2019) 25816–25827, https://doi.org/10.1073/pnas.1913491116.
[36] N. Kanagawa, M. Niwa, Y. Hatanaka, Y. Tani, S. Nakagawa, T. Fujita, A. Yamamoto, N. Okada, CC-chemokine ligand 17 gene therapy induces tumor regression through augmentation of tumor-infiltrating immune cells in a murine model of preexisting CT26 colon carcinoma, Int. J. Cancer. 121 (2007) 2013–2022, https://doi.org/10.1002/ijc.22908.
[37] A.N. Cornforth, G.J. Lee, A.W. Fowler, D.J. Carbonell, R.O. Dillman, Increases in serum TARC/CCL17 levels are associated with progression-free survival in advanced melanoma patients in response to dendritic cell-based immunotherapy, J. Clin. Immunol. 29 (2009) 657–664, https://doi.org/10.1007/s10875-009-9299-3.
[38] P. Berraondo, M.F. Sanmamed, M.C. Ochoa, I. Etxeberria, M.A. Aznar, J.L. Pérez-Gracia, M.E. Rodríguez-Ruiz, M. Ponz-Sarvise, E. Castañón, I. Melero, Cytokines in clinical cancer immunotherapy, Br. J. Cancer. 120 (2019) 6–15, https://doi.org/10.1038/s41416-018-0328-y.
[39] D.S. and J.G. Frelinger, Challenges and developing solutions for increasing the benefits of IL-2 treatment in tumor therapy, Expert Rev Clin Immunol. 10 (2014) 207–217. https://doi.org/10.1586/1744666X.2014.875856.Challenges.
[40] W. Lasek, R. Zagożdżon, M. Jakobisiak, Interleukin 12: Still a promising candidate for tumor immunotherapy?, Cancer Immunol. Immunother. 63 (2014) 419–435, https://doi.org/10.1007/s00262-014-1523-1.
[41] C. Burkart, A. Mukhopadhyay, S.A. Shirley, R.J. Connolly, J.H. Wright, A. Bahrami, J.S. Campbell, R.H. Pierce, D.A. Canton, Improving therapeutic efficacy of IL-12 intratumoral gene electrotransfer through novel plasmid design and modified parameters, Gene Ther. 25 (2018) 93–103, https://doi.org/10.1038/s41434-018-0006-y.
[42] L.G. Campana, I. Edhemovic, D. Soden, A.M. Perrone, M. Scarpa, L. Campanacci, M. Cemazar, S. Valpione, D. Miklavčič, S. Mocellin, E. Sieni, G. Sersa, Electrochemotherapy – Emerging applications technical advances, new indications, combined approaches, and multi-institutional collaboration, Eur. J. Surg. Oncol. 45 (2019) 92–102, https://doi.org/10.1016/j.ejso.2018.11.023.
[43] G. Sersa, J. Teissie, M. Cemazar, E. Signori, U. Kamensek, G. Marshall, D. Miklavcic, Electrochemotherapy of tumors as in situ vaccination boosted by immunogene electrotransfer, Cancer Immunol. Immunother. 64 (2015) 1315–1327, https://doi.org/10.1007/s00262-015-1724-2.
[44] M. Cemazar, T. Jarm, G. Sersa, Cancer Electrogene Therapy with Interleukin-12, Curr. Gene Ther. 10 (2010) 300–311, https://doi.org/10.2174/156652310791823425.
[45] L. Lambricht, A. Lopes, S. Kos, G. Sersa, V. Préat, G. Vandermeulen, Clinical potential of electroporation for gene therapy and DNA vaccine delivery, Expert Opin. Drug Deliv. 13 (2016) 295–310, https://doi.org/10.1517/17425247.2016.1121990.
[46] R. Heller, L.C. Heller, Gene Electrotransfer Clinical Trials, Elsevier Ltd (2015), https://doi.org/10.1016/bs.adgen.2014.10.006.
[47] S.I.S. Mosely, J.E. Prime, R.C.A. Sainson, J.O. Koopmann, D.Y.Q. Wang, D.M. Greenawalt, M.J. Ahdesmaki, R. Leyland, S. Mullins, L. Pacelli, D. Marcus, J. Anderton, A. Watkins, J.C. Ulrichsen, P. Brohawn, B.W. Higgs, M. McCourt, H. Jones, J.A. Harper, M. Morrow, V. Valge-Archer, R. Stewart, S.J. Dovedi, R.W. Wilkinson, Rational selection of syngeneic preclinical tumor models for immunotherapeutic drug discovery, Cancer Immunol. Res. 5 (2017) 29–41, https://doi.org/10.1158/2326-6066.CIR-16-0114.
[48] Y. Huang, C. Ma, Q. Zhang, J. Ye, F. Wang, Y. Zhang, P. Hunborg, M.A. Varvares, D.F. Hoft, E.C. Hsueh, G. Peng, CD4+ and CD8+ T cells have opposing roles in breast cancer progression and outcome, Oncotarget. 6 (2015) 17462–17478. 10.18632/oncotarget.3958.
[49] C.N. Johnstone, Y.E. Smith, Y. Cao, A.D. Burrows, R.S.N. Cross, X. Ling, R.P. Redvers, J.P. Doherty, B.L. Eckhardt, A.L. Natoli, C.M. Restall, E. Lucas, H.B. Pearson, S. Deb, K.L. Britt, A. Rizzitelli, J. Li, J.H. Harmey, N. Pouliot, R.L. Anderson, Functional and molecular characterisation of EO771.LMB tumours, a new C57BL/6-mouse-derived model of spontaneously metastatic mammary

cancer, DMM Dis, Model. Mech. 8 (2015) 237–251, https://doi.org/10.1242/dmm.017830.
[50] L.M. Mir, J. Gehl, G. Sersa, C.G. Collins, J.R. Garbay, V. Billard, P.F. Geertsen, Z. Rudolf, G.C. O'Sullivan, M. Marty, Standard operating procedures of the electrochemotherapy: Instructions for the use of bleomycin or cisplatin administered either systemically or locally and electric pulses delivered by the CliniporatorTM by means of invasive or non-invasive electrodes, Eur. J. Cancer, Suppl. 4 (2006) 14–25, https://doi.org/10.1016/j.ejcsup.2006.08.003.
[51] R. Dežman, M. Čemažar, G. Serša, A. Seliškar, V. Erjavec, B. Trotovšek, G. Gašljevič, M. Bošnjak, U. Lampreht Tratar, B. Kos, M. Djokić, N. Milevoj, M. Štukelj, N. Boc, J. Izlakar, P. Popovič, Safety and Feasibility of Electrochemotherapy of the Pancreas in a Porcine Model, Pancreas. 49 (2020) 1168–1173, https://doi.org/10.1097/MPA.0000000000001642.
[52] S.K. Greaney, A.P. Algazi, K.K. Tsai, K.T. Takamura, L. Chen, C.G. Twitty, L. Zhang, A. Paciorek, R.H. Pierce, M.H. Le, A.I. Daud, L. Fong, Intratumoral Plasmid IL12 Electroporation Therapy in Patients with Advanced Melanoma Induces Systemic and Intratumoral T-cell Responses, Cancer Immunol. Res. 8 (2020) 246–254, https://doi.org/10.1158/2326-6066.CIR-19-0359.
[53] A.P. Algazi, C.G. Twitty, K.K. Tsai, M. Le, R. Pierce, E. Browning, R. Hermiz, D.A. Canton, D. Bannavong, A. Oglesby, M. Francisco, L. Fong, M.J. Pittet, S.P. Arlauckas, C. Garris, L.P. Levine, C. Bifulco, C. Ballesteros-Merino, S. Bhatia, S. Gargosky, R.H.I. Andtbacka, B.A. Fox, M.D. Rosenblum, A.I. Daud, Phase II Trial of IL-12 Plasmid Transfection and PD-1 Blockade in Immunologically Quiescent Melanoma, Clin. Cancer Res. 26 (2020) 2827–2837, https://doi.org/10.1158/1078-0432.CCR-19-2217.
[54] T. Forjanic, B. Markelc, M. Marcan, E. Bellard, F. Couillaud, M. Golzio, D. Miklavcic, Electroporation-Induced Stress Response and Its Effect on Gene Electrotransfer Efficacy. In Vivo Imaging and Numerical Modeling, IEEE Trans. Biomed. Eng. 66 (2019) 2671–2683, https://doi.org/10.1109/TBME.2019.2894659.
[55] D.J. Langford, A.L. Bailey, M.L. Chanda, S.E. Clarke, T.E. Drummond, S. Echols, S. Glick, J. Ingrao, T. Klassen-Ross, M.L. Lacroix-Fralish, L. Matsumiya, R.E. Sorge, S.G. Sotocinal, J.M. Tabaka, D. Wong, A.M.J.M. Van Den Maagdenberg, M.D. Ferrari, K.D. Craig, J.S. Mogil, Coding of facial expressions of pain in the laboratory mouse, Nat. Methods. 7 (2010) 447–449, https://doi.org/10.1038/nmeth.1455.
[56] S.K. Brezar, M. Kranjc, M. Čemažar, S. Buček, G. Serša, D. Miklavčič, Electrotransfer of siRNA to silence enhanced green fluorescent protein in tumor mediated by a high intensity pulsed electromagnetic field, Vaccines. 8 (2020) 1–16, https://doi.org/10.3390/vaccines8010049.
[57] A. Masotti, G. Mossa, C. Cametti, G. Ortaggi, A. Bianco, N. Del Grosso, D. Malizia, C. Esposito, Comparison of different commercially available cationic liposome-DNA lipoplexes: Parameters influencing toxicity and transfection efficiency, Colloids Surfaces B Biointerfaces. 68 (2009) 136–144, https://doi.org/10.1016/j.colsurfb.2008.09.017.
[58] R.S. Sellers, Translating Mouse Models: Immune Variation and Efficacy Testing, Toxicol. Pathol. 45 (2017) 134–145, https://doi.org/10.1177/0192623316675767.
[59] L. Jacobs, E. De Smidt, N. Geukens, P. Declerck, K. Hollevoet, Electroporation outperforms in vivo-jetPEI for intratumoral DNA-based reporter gene transfer, Sci. Rep. 10 (2020) 1–5, https://doi.org/10.1038/s41598-020-75206-2.
[60] M. Bosnjak, B.C. Lorente, Z. Pogacar, V. Makovsek, M. Cemazar, Different incubation times of cells after gene Electrotransfer in fetal bovine serum affect cell viability, but not Transfection efficiency, J. Membr. Biol. 247 (2014) 421–428, https://doi.org/10.1007/s00232-014-9649-9.
[61] C. Rosazza, S.H. Meglic, A. Zumbusch, M.-P. Rols, D. Miklavcic, Gene Electrotransfer: A Mechanistic Perspective, Curr. Gene Ther. 16 (2016) 98–129. http://clinicaltrials.gov.
[62] V. Mlakar, V. Todorovic, M. Cemazar, D. Glavac, G. Sersa, Electric pulses used in electrochemotherapy and electrogene therapy do not significantly change the expression profile of genes involved in the development of cancer in malignant melanoma cells, BMC Cancer. 9 (2009) 299, https://doi.org/10.1186/1471-2407-9-299.
[63] E. Sieni, M. Dettin, M. De Robertis, B. Bazzolo, M.T. Conconi, A. Zamuner, R. Marino, F. Keller, L.G. Campana, E. Signori, The efficiency of gene electrotransfer in breast-cancer cell lines cultured on a novel collagen-free 3D scaffold, Cancers (Basel). 12 (2020), https://doi.org/10.3390/cancers12041043.
[64] M. De Robertis, L. Pasquet, L. Loiacono, E. Bellard, L. Messina, S. Vaccaro, R. Di Pasquale, V.M. Fazio, M.P. Rols, J. Teissie, M. Golzio, E. Signori, In vivo evaluation of a new recombinant hyaluronidase to improve gene electrotransfer protocols for dna-based drug delivery against cancer, Cancers (Basel). 10 (2018), https://doi.org/10.3390/cancers10110405.
[65] S. Luecke, A. Holleufer, M.H. Christensen, K.L. Jønsson, G.A. Boni, L.K. Sørensen, M. Johannsen, M.R. Jakobsen, R. Hartmann, S.R. Paludan, cGAS is activated by DNA in a length-dependent manner, EMBO Rep. 18 (2017) 1707–1715. 10.15252/embr.201744017.
[66] M. Motwani, S. Pesiridis, K.A. Fitzgerald, DNA sensing by the cGAS–STING pathway in health and disease, Nat. Rev. Genet. 20 (2019) 657–674, https://doi.org/10.1038/s41576-019-0151-1.
[67] K. Znidar, M. Bosnjak, M. Cemazar, L.C. Heller, Cytosolic DNA Sensor Upregulation Accompanies DNA Electrotransfer in B16.F10 Melanoma Cells, Mol. Ther. - Nucleic Acids. 5 (2016), https://doi.org/10.1038/mtna.2016.34 e322.
[68] K.J. MacKenzie, P. Carroll, C.A. Martin, O. Murina, A. Fluteau, D.J. Simpson, N. Olova, H. Sutcliffe, J.K. Rainger, A. Leitch, R.T. Osborn, A.P. Wheeler, M. Nowotny, N. Gilbert, T. Chandra, M.A.M. Reijns, A.P. Jackson, cGAS surveillance of micronuclei links genome instability to innate immunity, Nature. 548 (2017) 461–465, https://doi.org/10.1038/nature23449.
[69] J.F. Almine, C.A.J. O'Hare, G. Dunphy, I.R. Haga, R.J. Naik, A. Atrih, D.J. Connolly, J. Taylor, I.R. Kelsall, A.G. Bowie, P.M. Beard, L. Unterholzner, IFI16 and cGAS cooperate in the activation of STING during DNA sensing in human keratinocytes, Nat. Commun. 8 (2017), https://doi.org/10.1038/ncomms14392.
[70] L. Zhang, E. Nolan, S. Kreitschitz, D.P. Rabussay, Enhanced delivery of naked DNA to the skin by non-invasive in vivo electroporation, Biochim. Biophys. Acta - Gen. Subj. 1572 (2002) 1–9, https://doi.org/10.1016/S0304-4165(02)00270-2.
[71] G. Tevz, D. Pavlin, U. Kamensek, S. Kranjc, S. Mesojednik, A. Coer, G. Sersa, M. Cemazar, Gene electrotransfer into murine skeletal muscle: A systematic analysis of parameters for long-term gene expression, Technol. Cancer Res. Treat. 7 (2008) 91–101, https://doi.org/10.1177/153303460800700201.
[72] M. Cemazar, D. Pavlin, S. Kranjc, A. Grosel, S. Mesojednik, G. Sersa, Sequence and Time Dependence of Transfection Efficiency of Electrically- Assisted Gene Delivery to Tumors in Mice, Curr. Drug Deliv. 3 (2005) 77–81, https://doi.org/10.2174/156720106775197556.
[73] T. Batista Napotnik, D. Miklavčič, In vitro electroporation detection methods – An overview, Bioelectrochemistry. 120 (2018) 166–182, https://doi.org/10.1016/j.bioelechem.2017.12.005.
[74] S. Bhatia, N.V. Longino, N.J. Miller, R. Kulikauskas, J.G. Iyer, D. Ibrani, A. Blom, D. R. Byrd, U. Parvathaneni, C.G. Twitty, J.S. Campbell, M.H. Le, S. Gargosky, R.H. Pierce, R. Heller, A.I. Daud, P. Nghiem, Intratumoral delivery of plasmid IL12 via electroporation leads to regression of injected and noninjected tumors in Merkel cell carcinoma, Clin. Cancer Res. 26 (2020) 598–607, https://doi.org/10.1158/1078-0432.CCR-19-0972.
[75] F.M. André, J. Gehl, G. Sersa, V. Préat, P. Hojman, J. Eriksen, M. Golzio, M. Cemazar, N. Pavselj, M.P. Rols, D. Miklavcic, E. Neumann, J. Teissié, L.M. Mir, Efficiency of high- and low-voltage pulse combinations for gene electrotransfer in muscle, liver, tumor, and skin, Hum. Gene Ther. 19 (2008) 1261–1271, https://doi.org/10.1089/hum.2008.060.
[76] L. Heller, V. Todorovic, M. Cemazar, Electrotransfer of single-stranded or double-stranded DNA induces complete regression of palpable B16.F10 mouse melanomas, Cancer Gene Ther. 20 (2013) 695–700, https://doi.org/10.1038/cgt.2013.71.
[77] I.G. House, P. Savas, J. Lai, A.X.Y. Chen, A.J. Oliver, Z.L. Teo, K.L. Todd, M.A. Henderson, L. Giuffrida, E.V. Petley, K. Sek, S. Mardiana, T.N. Gide, C. Quek, R.A. Scolyer, G.V. Long, J.S. Wilmott, S. Loi, P.K. Darcy, P.A. Beavis, Macrophage-derived CXCL9 and CXCL10 are required for antitumor immune responses following immune checkpoint blockade, Clin. Cancer Res. 26 (2020) 487–504, https://doi.org/10.1158/1078-0432.CCR-19-1868.
[78] E.C. Keeley, B. Mehrad, R.M. Strieter, Chemokines as mediators of tumor angiogenesis and neovascularization, Exp. Cell Res. 317 (2011) 685–690, https://doi.org/10.1016/j.yexcr.2010.10.020.
[79] D. Peng, I. Kryczek, N. Nagarsheth, L. Zhao, S. Wei, W. Wang, Y. Sun, E. Zhao, L. Vatan, W. Szeliga, J. Kotarski, R. Tarkowski, Y. Dou, K. Cho, S. Hensley-Alford, A. Munkarah, R. Liu, W. Zou, Epigenetic silencing of TH1-type chemokines shapes tumour immunity and immunotherapy, Nature. 527 (2015) 249–253, https://doi.org/10.1038/nature15520.
[80] Y. Qin, S.N. Vasilatos, L. Chen, H. Wu, Z. Cao, Y. Fu, M. Huang, A.M. Vlad, B. Lu, S. Oesterreich, N.E. Davidson, Y. Huang, Inhibition of histone lysine-specific demethylase 1 elicits breast tumor immunity and enhances antitumor efficacy of immune checkpoint blockade, Oncogene. 38 (2019) 390–405, https://doi.org/10.1038/s41388-018-0451-5.
[81] K.G. Nguyen, M.R. Vrabel, S.M. Mantooth, J.J. Hopkins, E.S. Wagner, T.A. Gabaldon, D.A. Zaharoff, Localized Interleukin-12 for Cancer Immunotherapy, Front. Immunol. 11 (2020) 1–36, https://doi.org/10.3389/fimmu.2020.575597.
[82] U. Lampreht Tratar, L. Loiacono, M. Cemazar, U. Kamensek, V.M. Fazio, G. Sersa, E. Signori, Gene Electrotransfer of Plasmid-Encoding IL-12 Recruits the M1 Macrophages and Antigen-Presenting Cells Inducing the Eradication of Aggressive B16F10 Murine Melanoma, Mediators Inflamm. (2017 (2017).), https://doi.org/10.1155/2017/5285890.
[83] F. Castro, A.P. Cardoso, R.M. Gonçalves, K. Serre, M.J. Oliveira, Interferon-gamma at the crossroads of tumor immune surveillance or evasion, Front. Immunol. 9 (2018) 1–19, https://doi.org/10.3389/fimmu.2018.00847.
[84] N. Kumari, B.S. Dwarakanath, A. Das, A.N. Bhatt, Role of interleukin-6 in cancer progression and therapeutic resistance, Tumor Biol. 37 (2016) 11553–11572, https://doi.org/10.1007/s13277-016-5098-7.
[85] E.H. Cheteh, V. Sarne, S. Ceder, J. Bianchi, M. Augsten, H. Rundqvist, L. Egevad, A. Östman, K.G. Wiman, Interleukin-6 derived from cancer-associated fibroblasts attenuates the p53 response to doxorubicin in prostate cancer cells, Cell Death Discov. 6 (2020), https://doi.org/10.1038/s41420-020-0272-5.
[86] A. Sedlar, S. Kranjc, T. Dolinsek, M. Cemazar, A. Coer, G. Sersa, Radiosensitizing effect of intratumoral interleukin-12 gene electrotransfer in murine sarcoma, BMC Cancer. 13 (2013), https://doi.org/10.1186/1471-2407-13-38.
[87] G. Plavc, P. Strojan, Combining radiotherapy and immunotherapy in definitive treatment of head and neck squamous cell carcinoma: Review of current clinical trials, Radiol. Oncol. 54 (2020) 377–393, https://doi.org/10.2478/raon-2020-0060.